

We thank the reviewers for their constructive and helpful suggestions. We have provided our responses to the reviewers' comments and believe that our manuscript is much improved as a result.

The main paper improvements are:

- Section 2. Method was revised;
- More details regarding the NIES TM and FLEXPART modelling;
- Figures 7 and 10 are updated;

The reviewer's specific comments (shown in blue) are addressed below.

Anonymous Referee #1

Received and published: 23 July 2016

The authors presented a very interesting approach for selecting the colocated satellite XCO<sub>2</sub> retrievals according to the sensitivity footprint of each TCCON site. Overall the paper is well written, and should be published after minor revisions.

Major comments:

The authors used a trajectory model to calculate the sensitivity of a given TCCON observation (more exactly the boundary layer concentrations) to the emissions from neighbouring regions. Then they determined the 'footprint' of the TCCON site by choosing model cells with sensitivity above some predefined levels. My opinion is that such a simple definition may have some obvious issues:

1) Model cells with similar sensitivity do not necessarily make similar contributions to the observed TCCON column, because they can have some rather different emission/uptake strengths (for example one cell over ocean, and another may over land).

To take into account different emission/uptake strengths for different cell we use four types of a priori fluxes (anthropogenic, biosphere, and oceanic fluxes, as well as biomass burning emissions) optimized with the GELCA-EOF inverse modeling scheme (P5, L32).

2) The boundary layer concentrations are only part of the retrieved XCO<sub>2</sub> columns. As a result, the satellite XCO<sub>2</sub> observations selected according to the TCCON 'footprint' may still have large spread. I think as a result, there is no significant reduce in the standard deviation when compared to other approaches (Tables 4-8).

In this work we focused on study of the footprints of short-term variation in XCO<sub>2</sub> observed by TCCON and GOSAT. This variation is mainly managed by change of CO<sub>2</sub> concentration in boundary layer (Keppel-Aleks et al. 2012).

We think that the low accuracy of satellite observations ( $\pm 1$  ppm) is more important factor influenced on the results. Proposed method may have more benefits due to the use of more precise orbital instruments and improved retrieval algorithms.

Minor comments:

1. Line 2-3, Page 4: 'within  $\pm 30^\circ$  longitude,  $\pm 10^\circ$  latitude,  $\pm 5$  days, and  $\pm 2$  K of the selected TCCON location', As 5 days have been mentioned, 'location' may not be a proper word.

Revised as following:

“within  $\pm 30^\circ$  longitude,  $\pm 10^\circ$  latitude, and  $\pm 2$  K of the selected TCCON location and within  $\pm 5$  days window”

2. Line 11, Page 4: 'Limitations of the techinks !!!' Please delete it.

The paragraph “Bremen, Garmisch, Four Corners, JPL, and Izaña are influenced by local effects or complex terrain and are not included in averages (Kulawik ATM 2016). Limitations of the techinks !!!” was deleted.

3. Line 28, Page 8: 'dimensions of  $2.5^\circ \times 2.5^\circ$ ,  $\pm 5.0^\circ \times \pm 5.0^\circ$ , ...', Change  $2.5^\circ \times 2.5^\circ$

Disagree. For case C5 we use small box with size of  $2.5^\circ \times 2.5^\circ$ .

4. Line 3, Page 11: '...are within 0.81–0.93 ppm', remove 'ppm', as correlation coefficients have no unit.

Done

5. Line 13-15, Page 11: 'The dry season (May to September), the build-up season (high humidity, but little rain: October to December) and the wet season associated with tropical cyclones and monsoon rains (December to April).'

Not a complete sentence.

The paragraph revised as follows:

The Northern Territory of Australia has two distinctive climate zones: the northern and southern. The northern zone, including Darwin, has three distinct seasons: the dry season (May to September), the build-up season (high humidity, but little rain: October to December) and the wet season associated with tropical cyclones and monsoon rains (December to April). The average maximum temperature is remarkably similar all year round.

Anonymous Referee #2

Received and published: 2 June 2016

This manuscript presents a new method for selecting satellite data for validation against the ground-based TCCON sites. This method is based on calculated footprints that represent the sensitivity of the site to surrounding CO<sub>2</sub> concentrations. This new method is compared to simpler geographic-based data selection methods. This paper is methodologically sound but needs a few improvements in the description of the method, therefore, I recommend this manuscript for publication after minor changes have been made.

General comments

Method: more explanation of the FLEXPART modelling should be given. Specifically, which meteorological data were used, how the footprints are calculated and at what temporal and spatial resolution. Also, how the NIES TM model was used to initialize the FLEXPART simulations.

Whole section 2. Method was revised in order to provide more clear description.

The authors state that the TCCON observations are mostly sensitive to the lower troposphere, and that is why virtual particles were released at 1000 m. The authors however, do not take into account the vertical sensitivity of the TCCON measurements. What is the influence of assuming that the measurements are only sensitive to heights of circa 1000 m?

In this work we focused on study of the footprints of short-term (around one week) variation in XCO<sub>2</sub> observed by TCCON and GOSAT. This variation is mainly managed by change of CO<sub>2</sub> concentration in boundary layer (Keppel-Aleks et al. 2012).

Could the authors include a sensitivity test using multiple releases in FLEXPART to represent the averaging kernel?

Sensitivity test using multiple releases in FLEXPART to represent the averaging kernel is very expensive task, as it requires running trajectories for several months for the free troposphere and several years for the stratosphere. We have no available computational system to perform this task.

The colocation methods are compared for different GOSAT retrieval products. If the footprint-based method is considered the most comprehensive colocation method, would it be useful for also validating/assessing the different retrieval products by comparing these against the TCCON data. It would be interesting to include this comparison between

retrieval products in the manuscript. This would also make the manuscript of greater interest to the community.

Validating/assessing of the different retrieval products is a quit complicated and self-sufficient task, though we think such kind analysis is out of the scope of this manuscript. Moreover, recent papers cover this problem quit well: Oshchepkov, S., Bril, A., Yokota, T., Morino, I., Yoshida, Y., Matsunaga, T., Belikov, D. A., Wunch, D., Wennberg, P., Toon, G., O'Dell, C., Butz, A., Guerlet, S., Cogan, A., Bosch, H., Eguchi, N., Deutscher, N., Griffith, D., Macatangay, R., Notholt, J., Sussmann, R., Rettinger, M., Sherlock, V., Robinson, J., Kyro, E., Heikkinen, P., Feist, D. G., Nagahama, T., Kadygrov, N., Maksyutov, S., Uchino, O., and Watanabe, H.: Effects of atmospheric light scattering on spectroscopic observations of greenhouse gases from space. Part 2: Algorithm intercomparison in the GOSAT data processing for CO<sub>2</sub> retrievals over TCCON sites, *J. Geophys. Res.*, 118, doi: 10.1029/2012JD018782, 2013.

It is more reasonable to assess the different retrieval of OCO-2 products, as this instrument provides better coverage and larger number of observation points.

### Specific comments

P3, L4-8: Suggest adding the years when data are available from each satellite, e.g., SCIAMACHY was discontinued in 2012 and OCO-2 is only available since mid-2014.

Done

P3, L28-32: I suggest that the authors make it clear here that the region and time period selected is for selecting the satellite data, just to make it unambiguous.

Done

P4, L10-11: This sentence needs a bit more explanation. It should be stated that Bremen, Garmisch etc. are TCCON sites, and the acronym JPL should be explained. Also, it is not clear in which averages these sites are not included – is this a different method again, if so it needs explanation.

P4, L11-12: It looks here as though the authors forgot to remove their own comment?

Yes, it is true. The paragraph “Bremen, Garmisch, Four Corners, JPL, and Izaña are influenced by local effects or complex terrain and are not included in averages (Kulawik ATM 2016). Limitations of the techinks !!!” was deleted.

P5, L4-5: It is unclear how the CO<sub>2</sub> concentration fields from NIES TM are used to initialize the backward simulations with the LPDM. Also, the LPDM, FLEXPART, needs wind fields from e.g. meteorological reanalysis, which wind fields were used?

P5, L14-17: Firstly we run NIES TM for the target period (January 2010 to February 2011) using ten year's spin-up to ensure reduction of initialization errors. Then NIES TM CO<sub>2</sub> concentrations sampled at the location of TCCON sites at the level of 1 km above ground at 13:00 local time were used to initialize backward tracer simulations with the FLEXPART model.

P6, L7-8: Both models are driven by the Japanese Meteorological Agency Climate Data Assimilation System (JCDAS) datasets (Onogi et al., 2007).

P6, L11-14: It needs to be explained more clearly what the FLEXPART calculated footprints represent. Only from the figures is shown that the footprints are sensitivities to CO<sub>2</sub> concentrations (at 1 km?) and have units of ppm per umol/m<sup>2</sup>/s but this is not explained in the methods.

The FLEXPART calculated footprints represent the source-receptor relationship which is an important concept in air quality modelling. It describes the sensitivity of a “receptor” element  $y$  to a “source”  $x$ . The receptor could be, for example, the average concentration of a certain atmospheric trace substance in a given grid cell during a given time interval (P. Seibert and A. Frank, 2004). The traditional way of evaluating the footprint is to overlay the area with a grid and sum the footprint value of the particle touchdowns within each grid cell. Using this method, the footprint strongly depends on the selected grid spacing and on the number of particles released in the simulation (Kljun et al., 2002).

For more details please check the following papers:

Kljun, N., Rotach, M. W., and Schmid, H. P.: A 3D backward Lagrangian footprint model for a wide range of boundary layer stratifications, *Bound.-Layer Meteorol.* 103, 205–226, 2002.

Seibert P, Frank A.: Source-receptor matrix calculation with a Lagrangian particle dispersion model in backward mode, *Atmospheric Chemistry and Physics*, 23, 4(1), 51-63, 2004.

Is it true that the footprints can be understood to represent a type of averaging kernel of the CO<sub>2</sub> concentrations surrounding the site?

No. Footprint represents area to which observation site is sensitive.

Averaging kernels (AK) are a linear representation of the weighting of information content of retrieval parameters. AK related to the partition of information determined from the radiances and the prior information (usually a first guess) and usually employed for assessment of vertical information.

P8, L28: I think the authors mean “additional use of CO<sub>2</sub> observations”?

Disagree. CO observations are necessary to distinguish biosphere and anthropogenic fluxes.

P9, L24-29: Some clarification is perhaps needed here; cases C1-4 were using a cutoff limit of the footprint and cases C5-8 were standard geographical comparisons?

Yes, exactly.

P10, L12-13: While it is true that the bias is smallest with one observation, this could just be by chance? How significant are the differences between the biases?

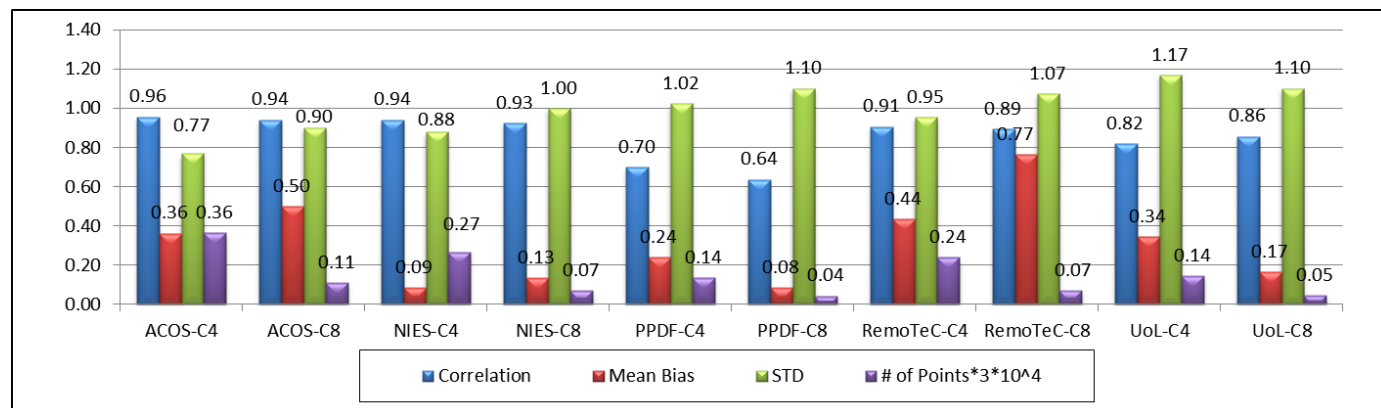
The difference between the two considered collocation methods is determined by the approaches to select spatial region around a TCCON site for selecting the satellite data. Case studies show how this spatial region may differ for cases 1-4 and 5-8. However, limited and uneven distribution of GOSAT data does not allow performing a more detailed analysis. Nevertheless, even a small reduction in a bias looks promising, as even a small bias can significantly affect the results of inverse modeling.

P11, L2: It's not clear what the authors mean by "collocation efficiency" if they mean the method, then there is a quite strong influence on the number of observations include in the comparison. Or do the author's rather mean that there is no dependence of the TCCON-GOSAT agreement on the collocation method?

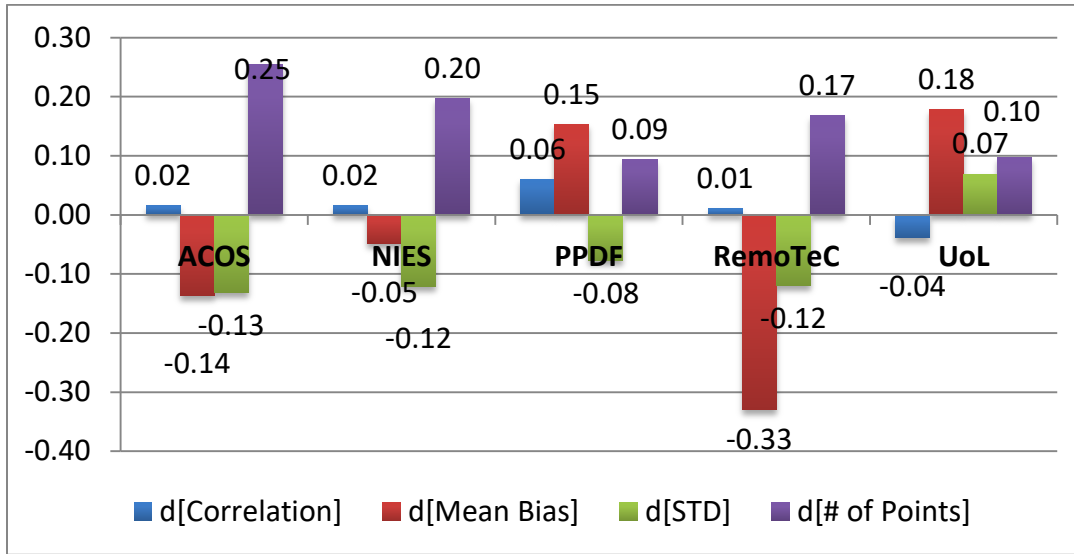
Here we stated that collocation efficiency doesn't depend on the number of observations include in the comparison.

Figure 7 and 10. By showing the difference between the two methods it is not clear which performs better. Instead it would be clearer and more meaningful to show these parameters (correlation etc.) for both methods.

Disagree. It is quite messy to show all these parameters (correlation etc.) for both methods. See below.



To make the figures more clear we added data labels:



It would also be helpful to briefly state again what each method is in the caption.

Done

Technical comments

P11, L1: please change to “differs by approximately a factor of 5”

Done



1                   **Study of the footprints of short-term variation in XCO<sub>2</sub> observed by TCCON**  
2                   **sites using NIES and FLEXPART atmospheric transport models**

3           **D.A. Belikov<sup>1,2,3,\*</sup>, S. Maksyutov<sup>1</sup>, A. Ganshin<sup>3,4</sup>, R. Zhuravlev<sup>3,4</sup>, N.M. Deutscher<sup>5,6</sup>,**  
4           **D. Wunch<sup>7</sup>, D.G. Feist<sup>8</sup>, I. Morino<sup>1</sup>, R. J. Parker<sup>9</sup>, K. Strong<sup>10</sup>, Y. Yoshida<sup>1</sup>, A. Bril<sup>11</sup>,**  
5           **S. Oshchepkov<sup>11</sup>, H.Boesch<sup>9</sup>, M. K. Dubey<sup>12</sup>, D. Griffith<sup>5</sup>, W. Hewson<sup>9</sup>, R. Kivi<sup>13</sup>, J.**  
6           **Mendonca<sup>10</sup>, J. Notholt<sup>6</sup>, M. Schneider<sup>14</sup>, R. Sussmann<sup>15</sup>, V.A. Velazco<sup>5</sup>, and S. Aoki<sup>16</sup>**

7 [1]{National Institute for Environmental Studies, Tsukuba, Japan}

8 [2]{National Institute of Polar Research, Tokyo, Japan}

9 [3]{Tomsk State University, Tomsk, Russia}

10 [4]{Central Aerological Observatory, Dolgoprudny, Russia}

11 [5]{Centre for Atmospheric Chemistry, School of Chemistry, University of Wollongong,  
12 Wollongong, NSW, Australia}

13 [6]{Institute of Environmental Physics, University of Bremen, Bremen, Germany}

14 [7]{California Institute of Technology, Pasadena, CA, USA}

15 [8]{Max Planck Institute for Biogeochemistry, Jena, Germany}

16 [9]{Earth Observation Science, University of Leicester, Leicester, UK}

17 [10]{Department of Physics, University of Toronto, Toronto, ON, Canada}

18 [11]{Institute of Physics of the National Academy of Sciences, Minsk, Belarus}

19 [12]{Earth System Observations, Los Alamos National Laboratory, Los Alamos, New Mexico}

20 [13]{Finnish Meteorological Institute, Sodankylä, Finland}

21 [14]{Agencia Estatal de Meteorología (AEMET), CIAI, Santa Cruz de Tenerife, Spain}

22 [15]{Karlsruhe Institute of Technology, IMK-IFU, Garmisch-Partenkirchen, Germany}

23 [16]{Tohoku University, Sendai, Japan}

24  
25 [\\* {Currently at Hokkaido University, Sapporo, Japan}](#)

26 Correspondence to: D. A. Belikov ([dmitry.belikov@nies.go.jp](mailto:dmitry.belikov@nies.go.jp))

27

## Abstract

The Total Carbon Column Observing Network (TCCON) is a network of ground-based Fourier Transform Spectrometers (FTS) that record near-infrared (NIR) spectra of the Sun. From these spectra, accurate and precise observations of CO<sub>2</sub> column-averaged dry-air mole fraction (denoted XCO<sub>2</sub>) are retrieved. TCCON FTS observations have previously been used to validate satellite estimations of XCO<sub>2</sub>; however, our knowledge of the short-term spatial and temporal variations in XCO<sub>2</sub> surrounding the TCCON sites is limited.

In this work, we use the National Institute for Environmental Studies (NIES) Eulerian three-dimensional transport model and the FLEXPART (FLEXible PARTicle) Lagrangian Particle Dispersion Model (LPDM) to determine the footprints of short-term variations in XCO<sub>2</sub> observed by operational, past, future, and possible TCCON sites. We propose a footprint-based method for the collocation of satellite and TCCON XCO<sub>2</sub> observations, and estimate the performance of the method using the NIES model and five GOSAT XCO<sub>2</sub> product datasets. Comparison of the proposed approach with a standard geographic method shows higher number of collocation points and average bias reduction up to 0.15 ppm for a subset of 16 stations for the period from January 2010 to January 2014. Case studies of the Darwin and La Réunion sites reveal that when the footprint area is rather curved, non-uniform and significantly different from a geographical rectangular area, the differences between these approaches are more noticeable. This emphasizes that the collocation is sensitive to local meteorological conditions and flux distributions.

**Keywords:** XCO<sub>2</sub>, TCCON, GOSAT, atmospheric transport

# 1. Introduction

Satellite observations of the column-averaged dry-air mole fraction of CO<sub>2</sub> (XCO<sub>2</sub>) have the potential to significantly advance our knowledge of carbon dioxide (CO<sub>2</sub>) distributions globally and provide new information on regional CO<sub>2</sub> sources and sinks. Observations of XCO<sub>2</sub> are available from space-based instruments such as the SCanning Imaging Absorption SpectroMeter for Atmospheric CHartographyY (SCIAMACHY; [data available for period 2002-2012](#); Bovensmann et al., 1999), the Greenhouse gases Observing Satellite (GOSAT; [data available since 2009](#); Kuze et al., 2009, 2016; Yokota et al., 2009), and the Orbiting Carbon Observatory-2 (OCO-2; [available since middle 2014](#); Crisp et al., 2004). These satellites provide unprecedented spatial coverage of the variability in XCO<sub>2</sub> around the world, with the exception of polar regions and areas with dense clouds. These observations are, however, limited by the orbit of the satellites, which typically measure in the local afternoon.

Ground-based Fourier Transform Spectrometer (FTS) observations available from the Total Carbon Column Observing Network (TCCON) (Wunch et al., 2011, [2015](#)) provide dense temporal resolution and are more precise and accurate than space-based instruments. However, the number of ground-based FTS sites is limited, with just 23 operational sites and several approved for the future. These sites are sparsely distributed, and Siberia, Africa, South America, and the oceans from middle to high latitudes are poorly covered. Despite this limitation, FTS observations are used to validate satellite retrievals in order to assess bias, variability, and other key parameters (e.g., Wunch et al., 2011; Lindqvist et al., 2015).

The spatial and temporal coverage of satellite observations over TCCON sites is sparse due to cloud and aerosol filters, retrieval selection criteria, and post-retrieval data quality filters. To obtain satellite observation data with small uncertainties it is necessary to apply a collocation method for aggregating neighboring soundings. Currently available methods for XCO<sub>2</sub> collocation include geographical (e.g., Cogan et al., 2012; Inoue et al., 2013; Reuter et al., 2013), T700 (it implies that the air with the same history of transport derived from the 700 hPa potential temperature has the same XCO<sub>2</sub>; Wunch et al., 2011), model-based (Guerlet et al., 2013), and geostatistical approaches (Nguyen et al., 2014).

In the geographical collocation method a spatial region around a TCCON site is selected together with a temporal window: [for selecting the satellite data](#). Inoue et al. (2013) used daily mean observations within a 10° × 10° area, Reuter et al. (2013) selected the monthly median of all observations within a 10° × 10° area, and Cogan et al. (2012) implemented narrower limits, using a two-hour mean period within a ±5° × ±5° area.

1 To increase the number of soundings, the spatial region may be expanded and additional  
2 selection criteria imposed. In the T700 collocation method proposed by Wunch et al. (2011),  
3 all observations within  $\pm 30^\circ$  longitude,  $\pm 10^\circ$  latitude,  ~~$\pm 5$  days~~, and  $\pm 2$  K of the selected TCCON  
4 location and within  $\pm 5$  days window are employed.

5 The model-based method proposed by Oshchepkov et al. (2012) and improved by  
6 Guerlet et al. (2013) uses daily mean values within 0.5 ppm of the 3 day-averaged model XCO<sub>2</sub>  
7 values and located within  $\pm 25^\circ$  longitude and  $\pm 7.5^\circ$  latitude of a TCCON site.

8 Nguyen et al. (2014) developed a geostatistical collocation methodology that selects  
9 observations using a “distance” function, which is a modified Euclidian distance in terms of  
10 latitude, longitude, time, and mid-tropospheric temperature at 700 hPa.

11 ~~Bremen, Garmisch, Four Corners, JPL, and Izaña are influenced by local effects or~~  
12 ~~complex terrain and are not included in averages (Kulawik ATM 2016). Limitations of the~~  
13 ~~techinks !!!~~

14 The majority of collocation methods described above have a common disadvantage; i.e.,  
15 they work with a rectangular spatial domain, which is convenient for technical handling but  
16 does not reflect the impact of surface sources or sinks of CO<sub>2</sub> and the local meteorology in the  
17 area of interest. The spatial domains in collocations should take into account these features to  
18 ensure that only appropriate observations are selected. Keppel-Aleks et al. (2011, 2012)  
19 showed that the largest gradient in XCO<sub>2</sub> is formed mainly by the north–south flux  
20 distribution, with variations in XCO<sub>2</sub> caused mainly by large-scale advection. TCCON and  
21 satellite XCO<sub>2</sub> observations have pronounced temporal variability and are thus important in  
22 studies of short-term variations in XCO<sub>2</sub>.

23 In this paper we study short-term variations in XCO<sub>2</sub> observed at TCCON sites. Although  
24 the XCO<sub>2</sub> is derived from column-averaged concentrations of CO<sub>2</sub>, XCO<sub>2</sub> observations are most  
25 sensitive to near-surface fluxes. The XCO<sub>2</sub> variations are thus related to changes in the CO<sub>2</sub>  
26 mole fraction occurring near the surface surrounding the TCCON sites (hereafter known as  
27 the footprints of the TCCON sites).

28 The remainder of this paper is organized as follows: an overview of the method for  
29 estimating the footprints of TCCON sites is presented in Section 2. The results of the footprint  
30 estimation and a new method for collocation are presented and discussed in Sections 3,4, and  
31 the conclusions are given in Section 5.

## 2. Method

To estimate the footprints of TCCON sites we used forward simulations employing the NIES Eulerian three-dimensional transport model (TM) and backward trajectory tracking using the FLEXPART LPDM model.

The key features of the NIES TM are as follows: a reduced horizontal latitude–longitude grid with a spatial resolution of  $2.5^\circ \times 2.5^\circ$  near the equator (Belikov et al., 2011); a vertical flexible hybrid sigma–isentropic ( $\sigma$ – $\theta$ ) grid with 32 levels up to the level of 5 hPa (Belikov et al., 2013b); separate parameterization of the turbulent diffusivity in the PBL and free troposphere (provided by the European Centre for Medium-Range Weather Forecasts (ECMWF) ERA-Interim reanalysis); and a modified Kuo-type parameterization scheme for cumulus convection (Belikov et al., 2013a).

The NIES model has previously been used to study the seasonal and inter-annual variability in  $\text{CO}_2$ . Belikov et al. (2013b) reported that the NIES model is able to successfully reproduce the vertical profile of  $\text{CO}_2$  as well as the seasonal and inter-annual variability in  $X\text{CO}_2$ . A comparison of modeled output with TCCON observations (Belikov et al., 2013b) revealed model biases of  $\pm 0.2\%$  for  $X\text{CO}_2$ ; on this basis we assume that the NIES TM is able to successfully reproduce the vertical profile of  $\text{CO}_2$  at the locations of TCCON sites.

Firstly we run NIES TM for the target period (January 2010 to February 2011) using ten year’s spin-up to ensure reduction of initialization errors. Then NIES TM  $\text{CO}_2$  concentrations sampled at the location of TCCON sites at the level of 1 km above ground at 13:00 local time were used to initialize backward tracer simulations with the FLEXPART model. FLEXPART, like other Lagrangian Particle Dispersion Models (LPDMs), considers atmospheric tracers as a discrete phase and tracks the pathway of each individual particle (Stohl et al., 2009). back in time until intersection with the Earth surface (Stohl et al., 2009). Obtained FLEXPART simulation results were then used to identify the areas in which TCCON soundings are most sensitive to variations.

The level of 1 km above ground typically corresponds to the top of the daytime planetary boundary layer (PBL). The PBL is the lowest part of the atmosphere and its behavior is directly influenced by its contact with the planetary surface. Turbulence causes intensive vertical mixing of the air within the PBL, so  $\text{CO}_2$  released from the surface is roughly uniformly distributed throughout the column of air in the PBL at local noon, when the maximum extent of vertical mixing occurs. The selected sampling time is also favorable for

1 minimizing errors in the initial CO<sub>2</sub> concentration calculated by NIES TM, as this type of  
2 chemical transport model has proved to be successful in resolving the diurnal vertical profiles  
3 of tracers (Belikov et al., 2013a).

4 To run NIES TM and FLEXPART model we use~~The NIES model has previously been used~~  
5 ~~to study the seasonal and inter-annual variability in CO<sub>2</sub>. Belikov et al. (2013b) reported that~~  
6 ~~the NIES model is able to successfully reproduce the vertical profile of CO<sub>2</sub> as well as the~~  
7 ~~seasonal and inter-annual variability in XCO<sub>2</sub>. A comparison of modeled output with TCCON~~  
8 ~~observations (Belikov et al., 2013b) revealed model biases of ±0.2% for XCO<sub>2</sub>; on this basis we~~  
9 ~~assume that the NIES TM is able to successfully reproduce the vertical profile of CO<sub>2</sub> at the~~  
10 ~~locations of TCCON sites.~~

11 ~~The key features of the NIES TM are as follows: a reduced horizontal latitude-longitude~~  
12 ~~grid with a spatial resolution of 2.5° × 2.5° near the equator (Belikov et al., 2011); a vertical~~  
13 ~~flexible hybrid sigma-isentropic ( $\sigma-\theta$ ) grid with 32 levels up to the level of 5 hPa (Belikov et~~  
14 ~~al., 2013b); separate parameterization of the turbulent diffusivity in the PBL and free~~  
15 ~~troposphere (provided by the European Centre for Medium-Range Weather Forecasts~~  
16 ~~(ECMWF) ERA-Interim reanalysis); and a modified Kuo-type parameterization scheme for~~  
17 ~~cumulus convection (Belikov et al., 2013a). The NIES TM was run using~~ fluxes obtained with  
18 the GELCA-EOF (Global Eulerian-Lagrangian Coupled Atmospheric model with Empirical  
19 Orthogonal Function) inverse modeling scheme (Zhuravlev et al., 2013). A priori fluxes  
20 consist of four types: 1) the Open source Data Inventory of Anthropogenic CO<sub>2</sub> (ODIAC) (Oda  
21 et al., 2011) and the Carbon Dioxide Information Analysis Center's (CDIAC) (Andres et al.,  
22 2011) anthropogenic fluxes; 2) the Vegetation Integrative Simulator for Trace gases (VISIT)  
23 (Ito, 2010) biosphere fluxes; 3) the Offline ocean Tracer Transport Model (OTTM) (Valsala et  
24 al., 2013) oceanic fluxes; and 4) the Global Fire Emissions Database (GFED) (Van der Werf et  
25 al., 2010) biomass burning emissions. The NIES and FLEXPARTBoth models are driven by the  
26 Japanese Meteorological Agency Climate Data Assimilation System (JCDAS) datasets (Onogi et  
27 al., 2007).

28 Variations in TCCON XCO<sub>2</sub> are influenced by a large spatial footprint scale processes.  
29 Keppel-Aleks et al. (2012) presented a robust relationship between weekly and monthly  
30 aggregated total column CO<sub>2</sub> and local net ecosystem exchange, while column drawdown has  
31 only a weak correlation with the regional flux on daily timescales. Thus the maximum  
32 trajectory duration for the model FLEXPART was therefore set to one week. The FLEXPART  
33 model was run to analyze TCCON site footprints with resolution of 1 degree and 2 h time step

1 | for a 14-month period from January 2010 to February 2011. ~~The FLEXPART model was then~~  
2 | ~~used to identify the areas in which TCCON soundings are most sensitive to variations on a~~  
3 | ~~short-term scale.~~

4

## 1 **3. Results**

### 2 **3.1. Sensitivity of TCCON site footprints**

3 We analyzed two groups of TCCON sites: operational sites (Table 1; Figs. 1 and 2) and  
4 past, future, and possible sites (Table 2; Fig. 3). We included Arrival Heights (Antarctica) and  
5 Yekaterinburg (Russia) in the second group, though the status of these monitoring stations is  
6 unclear. The footprint estimation is restricted to the summer season for high-latitude sites  
7 (Arrival Heights, Eureka, Ny Ålesund, Poker Flat, and Sodankylä), due to limitations relating to  
8 the solar zenith angle.

#### 9 *3.1.1. Operational sites*

##### 10 ***North America***

11 The five active American sites are located in the US and Canada, so they are sensitive to  
12 the western and central part of North America, the northern part of Canada and Greenland,  
13 and the eastern part of the Pacific Ocean. There are no TCCON sites in Alaska or on the east  
14 coast of North America, which is a region of intense anthropogenic activity (Fig. 1).

##### 15 ***European sites***

16 The European region contains eight operational sites (Fig. 2). We also include Izaña,  
17 which does not belong to this region but is located very close to it. This region has a good  
18 spatial coverage of operational TCCON sites; however, most sites are located near the coast  
19 and are thus very sensitive to the Atlantic and Arctic oceans. The maximum footprint  
20 sensitivity occurs in western Europe where there is a high density of operational TCCON sites;  
21 five sites (Bremen, Garmisch, Karlsruhe, Orléans, and Paris) are concentrated within a small  
22 area. The sensitivity decreases quite rapidly towards the east and south, and only parts of  
23 eastern Europe and north Africa are covered.

##### 24 ***Asia***

25 The footprints of Asian sites mainly span countries bordering the Sea of Japan; i.e., Japan,  
26 Korea, the Russian Far East, and east China. These sites are also able to capture signals from  
27 Mongolia, eastern Siberia, and Southeast Asia. Although the coverage of these sites is  
28 relatively small, the main industrial centers in the region are included.



## 1 ***Australia and New Zealand***

2 The footprint sensitivity of TCCON sites in this region covers almost all of Australia.  
3 Chevallier et al. (2011) shows TCCON data could constrain flux estimates over Australia  
4 equally well as the existing in situ measurements. Our footprint estimations are, however,  
5 more sensitive to the ocean regions between Australia and New Zealand as well as adjacent  
6 coastal areas.

## 7 ***Oceanic sites: Ascension Island and La Réunion Island***

8 Ascension Island is in the Trade Wind belt of the tropical Atlantic, ideally located to  
9 measure the South Atlantic marine boundary layer. The South East Trade Winds, which are  
10 almost invariant and are derived from the deep South Atlantic Ocean with little contact with  
11 Africa. Surface measurements of CO<sub>2</sub> at Ascension Island are used as a background (Gatti et al.,  
12 2010). However, above the Trade Wind Inversion (TWI), at about 1200–2000 m above sea  
13 level, the air masses are very different, coming dominantly from tropical Africa and  
14 occasionally South America (Swap et al., 1996). The FLEXPART simulation with tracers  
15 released at an altitude of 3000 m detected some hotspots in Africa (Fig. 1b). The study of  
16 biomass burning in Africa is essential, but lies outside of the scope of this paper.

17 La Réunion island situated in the Indian Ocean at about 800 km east of Madagascar. For  
18 this site the seasonal trend of wind mainly remains in the easterly sector, so the footprint  
19 covers mainly ocean regions. La Réunion site is further discussed in Section 4.3.2.

## 20 *3.1.2. Past, future, and possible TCCON sites*

21 The footprints of past, future, and possible TCCON sites are presented in Fig. 3. The  
22 Oxfordshire site enhances the sensitivity of the region, which is already well covered by  
23 existing TCCON sites in Europe. The East Trout Lake, Four Corners, and Poker Flat sites fill  
24 sensitivity gaps in the Canadian Boreal forest, the southwestern US, northern Mexico, and  
25 Alaska. Nevertheless, there are no TCCON sites near the Atlantic coast of North America,  
26 which is a key region of interest.

27 In South America, the Manaus site (briefly in operation during 2014 and will operate  
28 after reconstruction) was ideally located in central Amazonia. However, meteorological  
29 conditions meant that a signal was only detected in a very narrow section towards the east.  
30 Observations at this site are more sensitive to anthropogenic activity on the Atlantic coast of  
31 South America, compared with the surrounding Amazonian biosphere. Additional use of CO

1 observations will be necessary to isolate the Net Primary Production signal in Central  
2 Amazonia (Keppel-Aleks et al., 2012). Another site in this region is Paramaribo located in  
3 Suriname which is part of Caribbean South America. The footprint of the Paramaribo site is  
4 narrowly focused towards the Atlantic Ocean due to site location and meteorological  
5 conditions as stated above.

6 Burgos in the northern Philippines extends the Asian footprint southward. The location  
7 of the Yekaterinburg site is ideal, as it quite evenly covers a large area of western Russia. The  
8 site reduces the gap between the European and Asian TCCON domains. The Arrival Heights  
9 site is located on the Antarctic coast and currently cannot be used for satellite data validation.  
10 Given the air circulation near the South Pole, this site can be useful for measuring the  
11 background value of XCO<sub>2</sub>.

12 In general, the operational stations cover some regions well (North America, Europe, the  
13 Far East, Southeast Asia, Australia, and New Zealand), and the planned sites will improve this  
14 coverage. However, on a global scale there are major gaps that highlight the difficulty in  
15 generalizing the available data along latitude for bias correction.

16 The short-term variations in CO<sub>2</sub> in the near surface and free troposphere (<3000 m)  
17 have the same form, but different intensity (Fig. 1b), as a smaller number of tracers from the  
18 middle troposphere reached the surface during the simulation time.

### 19 **3.2. Seasonal variability in footprints**

20 Some TCCON stations have strong seasonal variations in their footprint due to changes  
21 in wind direction; i.e., Białystok, Darwin, Izaña, Park Falls, and Tsukuba (Fig. 4). For other  
22 sites (e.g., Ascension and Manaus) the weather conditions are less variable throughout the  
23 year. The depth of the PBL changes with season and is thus an important factor that influences  
24 the footprint. In winter the PBL lowers, causing less vertical mixing and enhancing horizontal  
25 tracer transport; this leads to a wider spatial coverage of the footprints.

## 26 **4. Applying the model-derived footprints to the collocation of XCO<sub>2</sub>**

27 In the next two sections we assess the performance of the footprint-based method of  
28 collocating TCCON XCO<sub>2</sub> against the NIES model and GOSAT product datasets. The collocation  
29 domain size for each site is determined by sensitivity values (ppm (μmol (m<sup>2</sup>s)<sup>-1</sup>)<sup>-1</sup>) with the  
30 limits of log<sub>10</sub>(x) equal to -0.5, -1.0, -1.5, and -2.0 (cases C1-C4). These sensitivity values  
31 were selected to approximately correspond to the domain sizes in standard geographical

1 colocation techniques, which have rectangular dimensions of  $2.5^\circ \times 2.5^\circ$ ,  $\pm 5.0^\circ \times \pm 5.0^\circ$ ,  $\pm 5.0^\circ \times$   
2  $\pm 10.0^\circ$ , and  $\pm 7.5^\circ \times \pm 22.5^\circ$  (cases C5-C8). Only coincident observations were used, and  
3 observations with differences of  $\geq 3$  ppm were discarded from the comparison. Considered  
4 period for comparison is January 2010 and January 2014.

5 TCCON observations were used from 16 sites: Białystok, Caltech, Darwin, Eureka,  
6 Garmisch, Izaña, Karlsruhe, Lamont, Lauder (125HR), Orléans, Park Falls, La Réunion Island,  
7 Saga, Sodankylä, Tsukuba (125HR), and Wollongong. These observations were obtained from  
8 the 2014 release of TCCON data (“GGG2014”), available from the TCCON Data Archive  
9 (<http://tcon.ornl.gov>).

#### 10 **4.1. Colocation of XCO<sub>2</sub> from TCCON and the NIES model**

11 The TCCON and NIES TM datasets are initially compared using a geographical colocation  
12 of  $2.5^\circ \times 2.5^\circ$  that corresponds to selecting the nearest NIES TM cell (Table 3). The resolution  
13 of the model grid is rather coarse, so we observe that the results depend mainly on the size of  
14 the colocation area but not on the form. With increasing size of the colocation area the  
15 correlation between XCO<sub>2</sub> from TCCON and NIES TM slightly increases from 0.96 to 0.97 and  
16 the standard deviation decreases from 1.1 to 0.96 ppm. This is due to an increase in the  
17 number of observations, which results in a larger average bias.

18 For Darwin, Eureka, Izaña, Lauder, La Réunion, Sodankylä, and Wollongong, the  
19 residuals between the datasets are small and similar for all methods (see Fig. 5a for Darwin;  
20 cases C1, C4, C5, and C8). Here, XCO<sub>2</sub> is under the influence of global long-term variations that  
21 are included in the NIES TM. The low sensitivity of the model to local sources does not cause a  
22 significant difference between the colocation methods. For the second group (non-operational  
23 sites), local sources are essential and even coarse-grid models can capture their signal. As a  
24 result, the shape of the colocation area is important (see Fig. 5b for Garmisch; cases C1, C4, C5,  
25 and C8).

#### 26 **4.2. Colocation of XCO<sub>2</sub> from TCCON and GOSAT products**

27 A comparison of colocation methods was performed for five GOSAT XCO<sub>2</sub> products: NIES  
28 v02.11 (Yoshida et al., 2013) and PPDF-S v02.11 from the NIES, Japan (Oshchepkov et al.,  
29 2013); ACOS B3.4 from the NASA Atmospheric CO<sub>2</sub> Observations from Space (ACOS) team  
30 (O’Dell et al., 2012); RemoTeC v2.11 from the Netherlands Institute for Space  
31 Research/Karlsruhe Institute of Technology, Germany (Butz et al., 2011; Guerlet et al., 2013);  
32 and UoL-FP v4 from the University of Leicester, UK (Boesch et al., 2011; Cogan et al., 2012).

1 The results of the comparison of eight collocation methods employed for the five GOSAT  
2 XCO<sub>2</sub> products are presented in Tables 4–8. Only coincident observations were used, and  
3 observations with differences of  $\geq 3$  ppm were discarded from the comparison. The number of  
4 observations selected for collocation between the methods with the smallest areas (C1 and C5)  
5 and largest areas (C4 and C8) differs by ~~about 5 times~~approximately a factor of 5. There is,  
6 however, no clear dependence of the collocation efficiency on the number of observations. The  
7 correlation coefficient and standard deviation are within 0.81–0.93 ~~ppm~~ and 1.02–1.22 ppm,  
8 respectively, regardless of the method used. Mean bias values are within 0.50–0.87 ppm, with  
9 the footprint method typically having a slightly lower bias by 0.02–0.15 ppm and higher  
10 number of collocations. For individual stations, these statistics may lie slightly outside the  
11 specified ranges.

### 12 4.3. Case study

13 In this section we demonstrate the developed collocation method for GOSAT  
14 observations over the Darwin and La Réunion Island TCCON sites.

#### 15 4.3.1. Darwin site

16 ~~Darwin lies in the~~The Northern Territory, ~~of~~ Australia, ~~which~~ has two distinctive climate  
17 zones: the northern and southern. The northern zone, including Darwin, has three distinct  
18 ~~wet and dry~~ seasons ~~and the average maximum temperature is remarkably similar all year~~  
19 ~~round. The:~~ the dry season (May to September), the build-up season (high humidity, but little  
20 rain: October to December) and the wet season associated with tropical cyclones and  
21 monsoon rains (December to April). The average maximum temperature is remarkably  
22 similar all year round. The southern zone is mainly desert with a semi-arid climate and little  
23 rain. To the north of Darwin, the territory is bordered by the Timor Sea, the Arafura Sea, and  
24 the Gulf of Carpentaria. The Northern Territory therefore has a pronounced seasonal  
25 variability that affects the spatial and temporal distribution of CO<sub>2</sub> and thus the footprint (Figs  
26 4 and 6a).

27 Figures 6b and 6c show the locations of GOSAT observations selected using a  
28 geographical method within an area of  $\pm 7.5^\circ \times \pm 22.5^\circ$  and a footprint-based method with the  
29 limit  $\log_{10}(x) = -2.0$ . Sizes of selected collocation areas (C4 and C8 methods) are close to ones  
30 used in others works (Wunch et al., 2011, Guerlet et al., 2013, Inoue et al. 2013, Reuter et al.  
31 2013, Nguyen et al., 2014).

1 For ACOS, NIES, and RemoTeC GOSAT products the distributions of XCO<sub>2</sub> datasets for the  
2 Darwin site are similar and cover an area to the west of Darwin, including ground-based  
3 observations from central Australia (Fig. 6c). The comparison of colocation methods shows  
4 the footprint-based method (C4) outperforms the geographical method (C8) for these three  
5 GOSAT products (Fig. 7), with approximately 3 times as many observations.

6 Although currently the UoL GOSAT XCO<sub>2</sub> version 6 includes ocean-glint observations, in  
7 this study we use slightly outdated the UoL-FP GOSAT product v4, which has only overland  
8 points. In this case the difference between colocations subsets is the observations towards the  
9 south over land, which provide a similar distribution as the ACOS product, but without marine  
10 observations (Fig. 6b and Fig. 6c). These differences in the covered areas have a significant  
11 negative effect on the result (Fig. 7). From that it can be concluded that XCO<sub>2</sub> patterns towards  
12 the south over land are rather different from those around Darwin, the sun-glint observation  
13 over the ocean are important and must be included into analysis. Thus, XCO<sub>2</sub> at the Darwin  
14 site is under the influence of the three different fluxes coming from surrounding land area,  
15 central part of Australia and oceanic regions. The oceanic observation over the Coral sea is  
16 quite important, though substantially removed from the station.

#### 17 4.3.2. *La Réunion site*

18 La Réunion is a small island east of Madagascar surrounded by the Indian Ocean. The  
19 nearest land territory to La Réunion is Mauritius, located ~175 km to the northwest. The  
20 meteorological conditions in the region mean that the footprint of the La Réunion site mostly  
21 covers a large area of ocean to the southeast of the island and a small area of northern  
22 Madagascar (Fig. 8).

23 The geographical colocation method does not take into account local conditions.  
24 Therefore, despite the fact that the site is predominantly oceanic, the geographical method  
25 includes observations made over land in Madagascar and the southeast coast of Africa (Fig.  
26 8b). In contrast, the footprint method takes into account the local meteorology, so  
27 observations are predominantly taken from the ocean (Fig. 8c). Since the UoL-FP dataset has  
28 no observations over the sea, the observations for this dataset are located only over  
29 Madagascar (Fig. 9).

30 Unlike Darwin, La Réunion receives clean air from the ocean and thus has very little CO<sub>2</sub>  
31 variation. The selection of areas for colocation therefore did not reveal any significant  
32 advantages of the footprint-based method, with the exception of a slightly smaller bias for the

1 NIES and RemoTec products (Fig. 10). The comparison of the UoL-FP product for method C4  
2 and method C8 shows that the XCO<sub>2</sub> cycles over Madagascar and the eastern coast of Africa  
3 are quite different (Fig. 10). This highlights that the exclusion of marine observations leads to  
4 poor results over marine-based TCCON sites.

5 A comparison of TCCON data and NIES model results for Darwin and La Réunion shows  
6 that XCO<sub>2</sub> for these sites is controlled mainly by large-scale changes. However, analysis of  
7 GOSAT products emphasizes that the influence of local sources is also important. The  
8 geographical method of collocation assumes a fairly even distribution of GOSAT observations  
9 near TCCON sites, while the calculated footprints have strongly curved shapes and an uneven  
10 distribution. We therefore expect the proposed footprint method to be useful for other sites  
11 with rather curved and non-uniform footprints, such as the Ascension Island and Manaus  
12 sites.

## 13 **5. Summary**

14 We have developed a method for assessing the footprints of short-term XCO<sub>2</sub> variations  
15 observed by TCCON ground-based FTS sites. The method is based on one-week FLEXPART  
16 backward trajectory simulations that are initiated at an altitude of 1 km (the upper border of  
17 the PBL) in the afternoon using the vertical CO<sub>2</sub> distribution calculated by the NIES transport  
18 model.

19 We applied this method to estimate footprints of the operational, past, future, and  
20 possible TCCON sites, and revealed some basic patterns. Most sites located near coastal  
21 regions are strongly influenced by ocean regions; thus, there is a large seasonal variability in  
22 footprints for Białystok, Darwin, Izaña, Park Falls, and Tsukuba. The Ascension Island,  
23 Manaus, and La Réunion sites have very narrow footprints that show small seasonal  
24 variations.

25 We proposed the footprint-based method for the collocation of satellite observations  
26 with TCCON sites, and assessed the performance of the method using the NIES model and  
27 GOSAT product datasets. The collocation footprint area is determined by yearly averaged  
28 sensitivity values with limits of  $\log_{10}(x)$  equals  $-0.5$ ,  $-1.0$ ,  $-1.5$  and  $-2.0$ . These were selected  
29 to approximately correspond to the areas of standard geographical collocation techniques that  
30 have rectangular shapes of  $2.5^\circ \times 2.5^\circ$ ,  $\pm 5.0^\circ \times \pm 5.0^\circ$ ,  $\pm 5.0^\circ \times \pm 10.0^\circ$ , and  $\pm 7.5^\circ \times \pm 22.5^\circ$ ,  
31 respectively. Comparison of the proposed method with the geographical method showed  
32 similar but smaller biases for a subset of 16 stations for the period from January 2009 to

1 January 2014. Case studies of the Darwin and La Réunion TCCON sites revealed that the  
2 footprint has a very different colocation area to that of the geographical method, especially  
3 near marine coast.

4 This study shows the use of colocation methods similar to geographical, which are based  
5 on tracking long-term trends of tracers (i.e. derived from global model calculations) has its  
6 limitations and works up to a certain accuracy threshold, after which it is impossible to ignore  
7 the influence of local sources. Given that the GOSAT XCO<sub>2</sub> products are sensitive to local  
8 sources, proposed footprint method is promising and requires further fine-tuning. The  
9 potential for further improvement includes moving from gross annual averaging to more  
10 accurate seasonal or monthly averaging. In addition, it is possible to study the sensitivity of  
11 XCO<sub>2</sub> observations using adjoint of the global Eulerian–Lagrangian coupled atmospheric  
12 transport model (Belikov et al., 2016), which can resolve long-term, synoptic and hourly  
13 variation patterns.

14 We believe, however, that the footprint analysis should be considered important in the  
15 appraisal of new TCCON sites, along with assessments of the number of cloudless days, the  
16 surrounding landscape, and the reflectivity of the Earth’s surface.

17

## Acknowledgments

Authors thank Paul Wennberg for insightful discussions and suggestions regarding the manuscript.

The JRA-25/JCDAS meteorological datasets used in the simulations were provided by the Japan Meteorological Agency. The computational resources were provided by NIES. This study was performed by order of the Ministry for Education and Science of the Russian Federation No. 5.628.2014/K and was supported by The Tomsk State University Academic D.I. Mendeleev Fund Program in 2014–2015 and by the GRENE Arctic project.

TCCON data were obtained from the TCCON Data Archive, hosted by the Carbon Dioxide Information Analysis Center (CDIAC; [tccon.ornl.gov](http://tccon.ornl.gov)).

[\) at Oak Ridge National Laboratory, Oak Ridge, Tennessee, U.S.A., http://tccon.ornl.gov.](http://tccon.ornl.gov)

The Ascension Island site has been funded by the Max Planck Society. The Bremen, Białystok, and Orléans TCCON sites are funded by the EU projects InGOS and ICOS-INWIRE, and by the Senate of Bremen. The Darwin and Wollongong TCCON sites are funded by NASA grants NAG5-12247 and NNG05-GD07G, and Australian Research Council grants DP140101552, DP110103118, DP0879468, LE0668470, and LP0562346. We are grateful to the DOE ARM program for technical support at the Darwin TCCON site. Nicholas Deutscher was supported by an Australian Research Council fellowship, DE140100178.

The Eureka measurements were made at the Polar Environment Atmospheric Research Laboratory (PEARL) by the Canadian Network for the Detection of Atmospheric Change (CANDAC) led by James R. Drummond, and in part by the Canadian Arctic ACE Validation Campaigns led by Kaley A. Walker. They were supported by the AIF/NSRIT, CFI, CFCAS, CSA, EC, GOC-IPY, NSERC, NSTP, OIT, ORF, and PCSP.

The University of Leicester data were obtained with funding from the UK National Centre for Earth Observation and the ESA GHG-CCI project, using the ALICE High Performance Computing Facility at the University of Leicester. R. Parker was funded by an ESA Living Planet Fellowship.



1  
2  
3  
4  
5  
6  
7  
8  
9  
10  
11  
12  
13  
14  
15  
16  
17  
18  
19  
20  
21  
22  
23  
24  
25  
26  
27  
28  
29  
30  
31  
32  
33  
34  
35  
36  
37  
38  
39  
40  
41  
42

## References

- Andres, R. J., Gregg, J. S., Losey, L., Marland, G., and Boden, T.: Monthly, global emissions of carbon dioxide from fossil fuel consumption, *Tellus*, 63B, 309–327, 2011.
- Belikov, D., Maksyutov, S., Miyasaka, T., Saeki, T., Zhuravlev, R., and Kiryushov, B.: Mass-conserving tracer transport modelling on a reduced latitude–longitude grid with NIES-TM, *Geosci. Model Dev.*, 4, 207–222, 2011.
- Belikov, D. A., Maksyutov, S., Krol, M., Fraser, A., Rigby, M., Bian, H., Agusti-Panareda, A., Bergmann, D., Bousquet, P., Cameron-Smith, P., Chipperfield, M. P., Fortems-Cheiney, A., Gloor, E., Haynes, K., Hess, P., Houweling, S., Kawa, S. R., Law, R. M., Loh, Z., Meng, L., Palmer, P. I., Patra, P. K., Prinn, R. G., Saito, R., and Wilson, C.: Off-line algorithm for calculation of vertical tracer transport in the troposphere due to deep convection, *Atmos. Chem. Phys.*, 13, 1093–1114, doi:10.5194/acp-13-1093-2013, 2013a.
- Belikov, D., Maksyutov, S., Sherlock, V., Aoki, S., Deutscher, N. M., Dohe, S., Griffith, D., Kyro, E., Morino, I., Nakazawa, T., Notholt, J., Rettinger, M., Schneider, M., Sussmann, R., Toon, G. C., Wennberg, P. O., and Wunch, D.: Simulations of column-average CO<sub>2</sub> and CH<sub>4</sub> using the NIES TM with a hybrid sigma–isentropic ( $\sigma$ – $\theta$ ) vertical coordinate, *Atmos. Chem. Phys.*, 13, 1713–1732, doi:10.5194/acp-13-1713-2013, 2013b.
- Belikov, D. A., Maksyutov, S., Yaremchuk, A., Ganshin, A., Kaminski, T., Blessing, S., Sasakawa, M., Gomez-Pelaez, A. J., and Starchenko, A.: Adjoint of the global Eulerian–Lagrangian coupled atmospheric transport model (A-GELCA v1.0): development and validation, *Geosci. Model Dev.*, 9, 749–764, doi:10.5194/gmd-9-749-2016, 2016.
- Boesch, H., Baker, D., Connor, B., Crisp, D., and Miller, C.: Global characterization of CO<sub>2</sub> column retrievals from shortwave-infrared satellite observations of the Orbiting Carbon Observatory-2 Mission, *Remote Sens.*, 3, 270–304, doi:10.3390/rs3020270, 2011.
- Bovensmann, H., Burrows, J. P., Buchwitz, M., Frerick, J., Noël, S., Rozanov, V. V., Chance, K. V., and Goede, A. P. H.: SCIAMACHY: Mission objectives and measurement modes, *J. Atmos. Sci.*, 56, 127–150, 1999.
- Butz, A., Guerlet, S., Jacob, D. J., Schepers, D., Galli, A., Aben, I., Frankenberg, C., Hartmann, J.-M., Tran, H., Kuze, A., Keppel-Aleks, G., Toon, G. C., Wunch, D., Wennberg, P. O., Deutscher, N. M., Griffith, D. W. T., Macatangay, R., Messerschmidt, J., Notholt, J., and Warneke, T.: Toward accurate CO<sub>2</sub> and CH<sub>4</sub> observations from GOSAT, *Geophys. Res. Lett.*, 38, 2–7, 2011.
- Chevallier, F., Deutscher, N. M., Conway, T. J., Ciais, P., Ciattaglia, L., Dohe, S., Frohlich, M., Gomez-Pelaez, A. J., Griffith, D., Hase, F., Haszpra, L., Krummel, P., Kyro, E., Labuschagne, C., Langenfelds, R., Machida, T., Maignan, F., Matsueda, H., Morino, I., Notholt, J., Ramonet, M., Sawa, Y., Schmidt, M., Sherlock, V., Steele, P., Strong, K., Sussmann, R., Wennberg, P., Wofsy, S., Worthy, D., Wunch, D., and Zimnoch, M.: Global CO<sub>2</sub> fluxes inferred from surface air-sample measurements and from TCCON retrievals of the CO<sub>2</sub> total column, *Geophys. Res. Lett.*, 38, L24810, doi:10.1029/2011GL049899, 2011

1 Cogan, A. J., Boesch, H., Parker, R. J., Feng, L., Palmer, P. I., Blavier, J.-F. L., Deutscher, N. M.,  
2 Macatangay, R., Notholt, J., Roehl, C., Warneke, T., and Wunch, D.: Atmospheric  
3 carbon dioxide retrieved from the Greenhouse gases Observing SATellite (GOSAT):  
4 Comparison with ground-based TCCON observations and GEOS-Chem model  
5 calculations, *J. Geophys. Res. Atmos.*, 117, D21301, doi:10.1029/2012JD018087, 2012.

6 Crisp, D., Atlas, R. M., Bréon, F.-M., Brown, L. R., Burrows, J. P., Ciais, P., Connor, B. J., Doney,  
7 S. C., Fung, I. Y., Jacob, D. J., Miller, C. E., O'Brien, D., Pawson, S., Randerson, J. T.,  
8 Rayner, P., Salawitch, R. S., Sander, S. P., Sen, B., Stephens, G. L., Tans, P. P., Toon, G.  
9 C., Wennberg, P. O., Wofsy, S. C., Yung, Y. L., Kuang, Z., Chudasama, B., Sprague, G.,  
10 Weiss, P., Pollock, R., Kenyon, D., and Schroll, S.: The Orbiting Carbon Observatory  
11 (OCO) mission, *Adv. Space Res.*, 34, 700–709, 2004.

12 Deutscher, N. M., Griffith, D. W. T., Bryant, G. W., Wennberg, P. O., Toon, G. C.,  
13 Washenfelder, R. A., Keppel-Aleks, G., Wunch, D., Yavin, Y., Allen, N. T., Blavier, J.-F.,  
14 Jiménez, R., Daube, B. C., Bright, A. V., Matross, D. M., Wofsy, S. C., and Park, S.: Total  
15 column CO<sub>2</sub> measurements at Darwin, Australia-site description and calibration against  
16 in situ aircraft profiles, *Atmos. Meas. Tech.*, 3, 947–958, doi:10.5194/amt-3-947-2010,  
17 2010.

18 Gatti, L. V., Miller, J. B., D'Amelio, M. T. S., Martinewski, A., Basso, L. S., Gloor, M. E., Wofsy,  
19 S., and Tans, P.: Vertical profiles of CO<sub>2</sub> above eastern Amazonia suggest a net carbon  
20 flux to the atmosphere and balanced biosphere between 2000 and 2009, *Tellus B*, 62,  
21 581–594, doi:10.1111/j.1600-0889.2010.00484.x, 2010.

22 Geibel, M. C., Gerbig, C., and Feist, D. G.: A new fully automated FTIR system for total  
23 column measurements of greenhouse gases, *Atmos. Meas. Tech.*, 3, 1363–1375,  
24 doi:10.5194/amt-3-1363-2010, 2010.

25 Guerlet, S., Butz, A., Schepers, D., Basu, S., Hasekamp, O. P., Kuze, A., Yokota, T., Blavier, J.-  
26 F., Deutscher, N. M., Griffith, D. W., Hase, F., Kyro, E., Morino, I., Sherlock, V.,  
27 Sussmann, R., Galli, A., and Aben, I.: Impact of aerosol and thin cirrus on retrieving and  
28 validating XCO<sub>2</sub> from GOSAT shortwave infrared measurements, *J. Geophys. Res.*  
29 *Atmos.*, 118, 4887–4905, 2013.

30 Inoue, M., Morino, I., Uchino, O., Miyamoto, Y., Yoshida, Y., Yokota, T., Machida, T., Sawa, Y.,  
31 Matsueda, H., Sweeney, C., Tans, P. P., Andrews, A. E., Biraud, S. C., Tanaka, T.,  
32 Kawakami, S., and Patra, P. K.: Validation of XCO<sub>2</sub> derived from SWIR spectra of GOSAT  
33 TANSO-FTS with aircraft measurement data, *Atmos. Chem. Phys.*, 13, 9771–9788,  
34 doi:10.5194/acp-13-9771-2013, 2013.

35 Ito, A.: Changing ecophysiological processes and carbon budget in East Asian ecosystems  
36 under near-future changes in climate: Implications for long-term monitoring from a  
37 process-based model, *J. Plant Res.*, 123, 577–588, 2010.

38 Keppel-Aleks, G., Wennberg, P. O., and Schneider, T.: Sources of variations in total column  
39 carbon dioxide, *Atmos. Chem. Phys.*, 11, 3581–3593, doi:10.5194/acp-11-3581-2011,  
40 2011.

41 Keppel-Aleks, G., Wennberg, P. O., Washenfelder, R. A., Wunch, D., Schneider, T., Toon, G.  
42 C., Andres, R. J., Blavier, J.-F., Connor, B., Davis, K. J., Desai, A. R., Messerschmidt, J.,  
43 Notholt, J., Roehl, C. M., Sherlock, V., Stephens, B. B., Vay, S. A., and Wofsy, S. C.: The

1 imprint of surface fluxes and transport on variations in total column carbon dioxide,  
2 Biogeosciences, 9, 875–891, doi:10.5194/bg-9-875-2012, 2012.

3 Kuze, A., Suto H., Nakajima M., and Hamazaki, T.: Thermal and near infrared sensor for  
4 carbon observation Fourier-transform spectrometer on the Greenhouse Gases  
5 Observing Satellite for greenhouse gases monitoring, Appl. Opt., 48, 6716–6733,  
6 doi:10.1364/AO.48.006716, 2009.

7 Kuze, A., suto, H., Shiomi, K., Kawakami, S., Tanaka, M., Ueda, Y., Deguchi, A., Yoshida, J.,  
8 Yamamoto, Y., Kataoka, F., Taylor, T. E., and Buijs, H.: Update on GOSAT TANSO-FTS  
9 performance, operations, and data products after more than six years in space, Atmos.  
10 Meas. Tech. Discuss., doi:10.5194/amt-2015-333, in review, 2016.

11 Lindqvist, H., O’Dell, C. W., Basu, S., Boesch, H., Chevallier, F., Deutscher, N., Feng, L., Fisher,  
12 B., Hase, F., Inoue, M., Kivi, R., Morino, I., Palmer, P. I., Parker, R., Schneider, M.,  
13 Sussmann, R., and Yoshida, Y.: Does GOSAT capture the true seasonal cycle of XCO<sub>2</sub>?,  
14 Atmos. Chem. Phys. Discuss., 15, 16461–16503, doi:10.5194/acpd-15-16461-2015,  
15 2015.

16 Messerschmidt, J., Macatangay, R., Notholt, J., Petri, C., Warneke, T., and Weinzierl, C.: Side  
17 by side measurements of CO<sub>2</sub> by ground-based Fourier transform spectrometry (FTS),  
18 Tellus B, 62, 749–758, doi:10.1111/j.1600-0889.2010.00491.x, 2010.

19 Messerschmidt, J., Chen, H., Deutscher, N. M., Gerbig, C., Grupe, P., Katrynski, K., Koch, F.-T.,  
20 Lavrič, J. V., Notholt, J., Rödenbeck, C., Ruhe, W., Warneke, T., and Weinzierl, C.:  
21 Automated ground-based remote sensing measurements of greenhouse gases at the  
22 Białystok site in comparison with collocated in situ measurements and model data,  
23 Atmos. Chem. Phys., 12, 6741–6755, doi:10.5194/acp-12-6741-2012, 2012.

24 Nguyen, H., Osterman, G., Wunch, D., O’Dell, C., Mandrake, L., Wennberg, P., Fisher, B., and  
25 Castano, R.: A method for collocating satellite XCO<sub>2</sub> data to ground-based data and its  
26 application to ACOS-GOSAT and TCCON, Atmos. Meas. Tech., 7, 2631–2644,  
27 doi:10.5194/amt-7-2631-2014, 2014.

28 Oda, T. and Maksyutov, S.: A very high-resolution (1 km × 1 km) global fossil fuel CO<sub>2</sub>  
29 emission inventory derived using a point source database and satellite observations of  
30 nighttime lights, Atmos. Chem. Phys., 11, 543–556, doi:10.5194/acp-11-543-2011,  
31 2011.

32 O’Dell, C. W., Connor, B., Bösch, H., O’Brien, D., Frankenberg, C., Castano, R., Christi, M.,  
33 Eldering, D., Fisher, B., Gunson, M., McDuffie, J., Miller, C. E., Natraj, V., Oyafuso, F.,  
34 Polonsky, I., Smyth, M., Taylor, T., Toon, G. C., Wennberg, P. O., and Wunch, D.: The  
35 ACOS CO<sub>2</sub> retrieval algorithm – Part 1: Description and validation against synthetic  
36 observations, Atmos. Meas. Tech., 5, 99–121, doi:10.5194/amt-5-99-2012, 2012.

37 Ohyama, H., Morino, I., Nagahama, T., Machida, T., Suto, H., Oguma, H., Sawa, Y., Matsueda,  
38 H., Sugimoto, N., Nakane, H., and Nakagawa, K.: Column-averaged volume mixing ratio  
39 of CO<sub>2</sub> measured with ground-based Fourier transform spectrometer at Tsukuba, J.  
40 Geophys. Res., 114, D18303, doi:10.1029/2008JD011465, 2009.

41 Onogi, K., Tsutsui, J., Koide, H., Sakamoto, M., Kobayashi, S., Hatsushika, H., Matsumoto, T.,  
42 Yamazaki, N., Kamahori, H., Takahashi, K., Kadokura, S., Wada, K., Kato, K., Oyama, R.,

1 Ose, T., Mannoji, N., and Taira, R.: The JRA-25 Reanalysis, *J. Meteor. Soc. Japan*, 85,  
2 369–432, 2007.

3 Oshchepkov, S., Bril, A., Yokota, T., Morino, I., Yoshida, Y., Matsunaga, T., Belikov, D., Wunch,  
4 D., Wennberg, P. O., Toon, G. C., O'Dell, C. W., Butz, A., Guerlet, S., Cogan, A., Boesch,  
5 H., Eguchi, N., Deutscher, N. M., Griffith, D., Macatangay, R., Notholt, J., Sussmann, R.,  
6 Rettinger, M., Sherlock, V., Robinson, J., Kyrö, E., Heikkinen, P., Feist, D. G., Nagahama,  
7 T., Kadyrov, N., Maksyutov, S., Uchino, O., and Watanabe, H.: Effects of atmospheric  
8 light scattering on spectroscopic observations of greenhouse gases from space:  
9 Validation of PPDF-based CO<sub>2</sub> retrievals from GOSAT, *J. Geophys. Res.*, 117, 1–18,  
10 2012.

11 Oshchepkov, S., Bril, A., Yokota, T., Yoshida, Y., Blumenstock, T., Deutscher, N. M., Dohe, S.,  
12 Macatangay, R., Morino, I., Notholt, J., Rettinger, M., Petri, C., Schneider, M., Sussman,  
13 R., Uchino, O., Velazco, V., Wunch, D., and Belikov, D.: Simultaneous retrieval of  
14 atmospheric CO<sub>2</sub> and light path modification from space-based spectroscopic  
15 observations of greenhouse gases: methodology and application to GOSAT  
16 measurements over TCCON sites, *Appl. Optics*, 52, 1339–1350, 2013.

17 Patra, P. K., Houweling, S., Krol, M., Bousquet, P., Belikov, D., Bergmann, D., Bian, H.,  
18 Cameron-Smith, P., Chipperfield, M. P., Corbin, K., Fortems-Cheiney, A., Fraser, A.,  
19 Gloor, E., Hess, P., Ito, A., Kawa, S. R., Law, R. M., Loh, Z., Maksyutov, S., Meng, L.,  
20 Palmer, P. I., Prinn, R. G., Rigby, M., Saito, R., and Wilson, C.: TransCom model  
21 simulations of CH<sub>4</sub> and related species: linking transport, surface flux and chemical loss  
22 with CH<sub>4</sub> variability in the troposphere and lower stratosphere, *Atmos. Chem. Phys.*,  
23 11, 12813–12837, doi:10.5194/acp-11-12813-2011, 2011.

24 Reuter, M., Bösch, H., Bovensmann, H., Bril, A., Buchwitz, M., Butz, A., Burrows, J. P., O'Dell,  
25 C. W., Guerlet, S., Hasekamp, O., Heymann, J., Kikuchi, N., Oshchepkov, S., Parker, R.,  
26 Pfeifer, S., Schneising, O., Yokota, T., and Yoshida, Y.: A joint effort to deliver satellite  
27 retrieved atmospheric CO<sub>2</sub> concentrations for surface flux inversions: the ensemble  
28 median algorithm EMMA, *Atmos. Chem. Phys.*, 13, 1771–1780, doi:10.5194/acp-13-  
29 1771-2013, 2013.

30 Stohl, A., Seibert, P., Arduini, J., Eckhardt, S., Fraser, P., Grealley, B. R., Lunder, C., Maione, M.,  
31 Mhle, J., O'Doherty, S., Prinn, R. G., Reimann, S., Saito, T., Schmidbauer, N., Simmonds,  
32 P. G., Vollmer, M. K., Weiss, R. F., and Yokouchi, Y.: An analytical inversion method for  
33 determining regional and global emissions of greenhouse gases: Sensitivity studies and  
34 application to halocarbons, *Atmos. Chem. Phys.*, 9, 1597–1620, doi:10.5194/acp-9-  
35 1597-2009, 2009.

36 Swap, R., Garstang, M., Macko, S. A., Tyson, P. D., Maenhaut, W., Artaxo, P., Kållberg, P., and  
37 Talbot R.: The long-range transport of southern African aerosols to the tropical South  
38 Atlantic, *J. Geophys. Res.*, 101(D19), 23777–23791, doi:10.1029/95JD01049, 1996.

39 Valsala, V., and Maksyutov, S.: Interannual variability of the air–sea CO<sub>2</sub> flux in the north  
40 Indian Ocean, *Ocean Dynam.*, 63, 165–178, doi:10.1007/s10236-012-0588-7, 2013.

41 Van der Werf, G. R., Randerson, J. T., Giglio, L., Collatz, G. J., Mu, M., Kasibhatla, P. S.,  
42 Morton, D. C., DeFries, R. S., Jin, Y., and Van Leeuwen, T. T.: Global fire emissions and

1 the contribution of deforestation, savanna, forest, agricultural, and peat fires (1997–  
2 2009), *Atmos. Chem. Phys.*, 10, 11707–11735, doi:10.5194/acp-10-11707-2010, 2010.  
3 Washenfelder, R., Toon, G., Blavier, J., Yang, Z., Allen, N., Wennberg, P., Vay, S., Matross, D.,  
4 and Daube, B.: Carbon dioxide column abundances at the Wisconsin Tall Tower site, *J.*  
5 *Geophys. Res.*, 111, D22305, doi:10.1029/2006JD007154, 2006.  
6 Wunch, D., Toon, G.C., Blavier, J.-F.L., Washenfelder, R.A., Notholt, J., Connor, B.J., Griffith,  
7 D.W.T., Sherlock, V., and Wennberg, P.O.: The Total Carbon Column Observing  
8 Network, *Phil. Trans. R. Soc. A* 369, 2087–2112, doi:10.1098/rsta.2010.0240, 2011.  
9 [Wunch, D., Toon, G.C, Sherlock, V., Deutscher, N.M., Liu, C., Feist, D.G., and Wennberg, P.O.](#)  
10 [The Total Carbon Column Observing Network’s GGG2014 Data Version. Technical](#)  
11 [report, Carbon Dioxide Information Analysis Center, Oak Ridge National Laboratory,](#)  
12 [Oak Ridge, Tennessee, U.S.A., 2015.](#)  
13 [doi:10.14291/tccon.ggg2014.documentation.R0/1221662.](#)  
14 Yokota, T., Yoshida, Y., Eguchi, N., Ota, Y., Tanaka, T., Watanabe, H., and Maksyutov, S.:  
15 Global concentrations of CO<sub>2</sub> and CH<sub>4</sub> retrieved from GOSAT: First preliminary results,  
16 *SOLA*, 5, 160–163, doi:10.2151/sola.2009-041, 2009.  
17 Yoshida, Y., Kikuchi, N., Morino, I., Uchino, O., Oshchepkov, S., Bril, A., Saeki, T., Schutgens,  
18 N., Toon, G. C., Wunch, D., Roehl, C. M., Wennberg, P. O., Griffith, D. W. T., Deutscher,  
19 N. M., Warneke, T., Notholt, J., Robinson, J., Sherlock, V., Connor, B., Rettinger, M.,  
20 Sussmann, R., Ahonen, P., Heikkinen, P., Kyrö, E., Mendonca, J., Strong, K., Hase, F.,  
21 Dohe, S., and Yokota, T.: Improvement of the retrieval algorithm for GOSAT SWIR XCO<sub>2</sub>  
22 and XCH<sub>4</sub> and their validation using TCCON data, *Atmos. Meas. Tech.*, 6, 1533–1547,  
23 doi:10.5194/amt-6-1533-2013, 2013.  
24 Zhuravlev, R.V., Ganshin, A.V., Maksyutov, S.S., Oshchepkov, S.L., Khattatov, B.V.: Estimation  
25 of global fluxes of CO<sub>2</sub> using ground-station and satellite (GOSAT) observation data  
26 with empirical orthogonal functions. *Atmos. Oceanic Opt.*, 26, 388-397, 2013.  
27

1 **Table 1.** Details of operational TCCON sites.

Number	Site	Latitude (Degrees)	Longitude (Degrees)	Altitude (km)
1	Anmyeondo, Korea	36.54	126.33	0.03
2	Ascension Island	7.92	-14.33	0.03
3	Białystok, Poland	53.23	23.03	0.18
4	Bremen, Germany	53.10	8.85	0.03
5	Caltech, USA	34.14	-118.13	0.23
6	Darwin, Australia	-12.42	130.89	0.03
7	Edwards, USA	34.96	-117.88	0.70
8	Eureka, Canada	80.05	-86.42	0.61
9	Garmisch, Germany	47.48	11.06	0.74
10	Izaña, Tenerife	28.30	-16.50	2.37
11	Karlsruhe, Germany	49.10	8.44	0.12
12	Lamont, USA	36.60	-97.49	0.32
13	Lauder, New Zealand	-45.04	169.68	0.37
14	Ny Ålesund, Spitsbergen	78.90	11.90	0.02
15	Orléans, France	47.97	2.11	0.13
16	Park Falls, USA	45.95	-90.27	0.44
17	Paris, France	48.85	2.32	0.10
18	La Réunion Island, France	-20.90	55.49	0.09
19	Rikubetsu, Japan	43.46	143.77	0.36
20	Saga, Japan	33.24	130.29	0.01
21	Sodankylä, Finland	67.37	26.63	0.19
22	Tsukuba, Japan	36.05	140.12	0.03
23	Wollongong, Australia	-34.41	150.88	0.03

2

3 **Table 2.** Past, future, and possible TCCON sites.

Number	Site	Latitude (Degrees)	Longitude (Degrees)	Altitude (km)
1	Arrival Heights, Antarctica	-77.83	166.66	0.25
2	Burgos, Philippines	18.50	120.85	0.10
3	East Trout Lake, Canada	54.35	-104.98	0.49
4	Four Corners, USA	36.80	-108.48	1.64
5	Manaus, Brazil	-3.10	-60.02	0.09
6	Oxfordshire, UK	51.57	-1.32	0.07
7	Paramaribo, Suriname	5.80	-55.20	0.05
8	Poker Flat, USA	65.12	-147.47	0.21
9	Yekaterinburg, Russia	57.04	59.55	0.30

4

1 **Table 3.** Averaged results of different collocation methods implemented for XCO<sub>2</sub> from NIES TM  
 2 calculated for 16 TCCON sites. \*The number of FLEXPART cells with resolution 1.0° × 1.0° is counted  
 3 for methods based on the footprint (1–4), while for other methods NIES TM cells (2.5° × 2.5°) are  
 4 used.

Case	Method of collocation	Mean number of cells*	Mean correlation coefficient	Absolute value of mean bias	Mean standard deviation
C1	Footprint limit $\log_{10}(x) = -0.5$	35	0.96	0.75	1.01
C2	Footprint limit $\log_{10}(x) = -1.0$	160	0.96	0.81	0.98
C3	Footprint limit $\log_{10}(x) = -1.5$	507	0.97	0.85	0.97
C4	Footprint limit $\log_{10}(x) = -2.0$	1071	0.97	0.88	0.96
C5	Within area of 2.5° × 2.5°	1	0.96	0.76	1.03
C6	Within area of ±5.0° × ±5.0°	16	0.96	0.79	1.00
C7	Within area of ±5.0° × ±10.0°	32	0.96	0.79	0.98
C8	Within area of ±7.5° × ±22.5°	108	0.97	0.80	0.97

5

6 **Table 4.** Averaged results of different collocation methods implemented for XCO<sub>2</sub> from the GOSAT  
 7 ACOS product calculated for 16 TCCON sites.

Case	Method of collocation	Mean number of observations	Mean correlation coefficient	Absolute value of mean bias	Mean standard deviation
C1	Footprint limit $\log_{10}(x) = -0.5$	1190	0.93	0.65	1.18
C2	Footprint limit $\log_{10}(x) = -1.0$	3046	0.92	0.61	1.21
C3	Footprint limit $\log_{10}(x) = -1.5$	4880	0.93	0.62	1.15
C4	Footprint limit $\log_{10}(x) = -2.0$	6016	0.93	0.64	1.12
C5	Within area of 2.5° × 2.5°	976	0.93	0.81	1.11
C6	Within area of ±5.0° × ±5.0°	2042	0.92	0.67	1.19
C7	Within area of ±5.0° × ±10.0°	3111	0.92	0.65	1.19
C8	Within area of ±7.5° × ±22.5°	5002	0.93	0.64	1.16

8

9

1 **Table 5.** Averaged results of different collocation methods implemented for XCO<sub>2</sub> from the GOSAT  
 2 NIES product calculated for 16 TCCON sites.

Case	Method of collocation	Mean number of observations	Mean correlation coefficient	Absolute value of mean bias	Mean standard deviation
C1	Footprint limit $\log_{10}(x) = -0.5$	1049	0.89	0.63	1.14
C2	Footprint limit $\log_{10}(x) = -1.0$	2890	0.92	0.52	1.20
C3	Footprint limit $\log_{10}(x) = -1.5$	4823	0.92	0.60	1.19
C4	Footprint limit $\log_{10}(x) = -2.0$	5922	0.92	0.56	1.16
C5	Within area of $2.5^\circ \times 2.5^\circ$	907	0.89	0.63	1.17
C6	Within area of $\pm 5.0^\circ \times \pm 5.0^\circ$	1845	0.91	0.56	1.15
C7	Within area of $\pm 5.0^\circ \times \pm 10.0^\circ$	2976	0.93	0.58	1.15
C8	Within area of $\pm 7.5^\circ \times \pm 22.5^\circ$	4874	0.92	0.60	1.17

3  
 4 **Table 6.** Averaged results of different collocation methods implemented for XCO<sub>2</sub> from the GOSAT  
 5 PPDF product calculated for 16 TCCON sites.

Case	Method of collocation	Mean number of observations	Mean correlation coefficient	Absolute value of mean bias	Mean standard deviation
C1	Footprint limit $\log_{10}(x) = -0.5$	357	0.84	0.50	1.11
C2	Footprint limit $\log_{10}(x) = -1.0$	870	0.86	0.62	1.12
C3	Footprint limit $\log_{10}(x) = -1.5$	1536	0.81	0.73	1.16
C4	Footprint limit $\log_{10}(x) = -2.0$	1911	0.81	0.67	1.17
C5	Within area of $2.5^\circ \times 2.5^\circ$	331	0.86	0.66	1.02
C6	Within area of $\pm 5.0^\circ \times \pm 5.0^\circ$	749	0.85	0.64	1.15
C7	Within area of $\pm 5.0^\circ \times \pm 10.0^\circ$	1114	0.83	0.69	1.19
C8	Within area of $\pm 7.5^\circ \times \pm 22.5^\circ$	1733	0.86	0.68	1.17

6  
 7 **Table 7.** Averaged results of different collocation methods implemented for XCO<sub>2</sub> from the GOSAT  
 8 RemoTeC product calculated for 16 TCCON sites.

Case	Method of collocation	Mean number of observations	Mean correlation coefficient	Absolute value of mean bias	Mean standard deviation
C1	Footprint limit $\log_{10}(x) = -0.5$	795	0.81	0.71	1.17
C2	Footprint limit $\log_{10}(x) = -1.0$	1898	0.83	0.66	1.19
C3	Footprint limit $\log_{10}(x) = -1.5$	3212	0.83	0.61	1.22
C4	Footprint limit $\log_{10}(x) = -2.0$	4091	0.83	0.59	1.21
C5	Within area of $2.5^\circ \times 2.5^\circ$	769	0.90	0.87	1.15
C6	Within area of $\pm 5.0^\circ \times \pm 5.0^\circ$	1491	0.85	0.63	1.18
C7	Within area of $\pm 5.0^\circ \times \pm 10.0^\circ$	2325	0.86	0.70	1.19
C8	Within area of $\pm 7.5^\circ \times \pm 22.5^\circ$	3818	0.86	0.64	1.25



1 **Table 8.** Averaged results of different collocation methods implemented for XCO<sub>2</sub> from the GOSAT  
 2 UoL-FP product calculated for 16 TCCON sites.

Case	Method of collocation	Mean number of observations	Mean correlation coefficient	Absolute value of mean bias	Mean standard deviation
C1	Footprint limit $\log_{10}(x) = -0.5$	634	0.88	0.78	1.31
C2	Footprint limit $\log_{10}(x) = -1.0$	1454	0.87	0.76	1.34
C3	Footprint limit $\log_{10}(x) = -1.5$	2450	0.88	0.80	1.28
C4	Footprint limit $\log_{10}(x) = -2.0$	3017	0.89	0.70	1.23
C5	Within area of $2.5^\circ \times 2.5^\circ$	629	0.86	0.73	1.33
C6	Within area of $\pm 5.0^\circ \times \pm 5.0^\circ$	1215	0.88	0.76	1.30
C7	Within area of $\pm 5.0^\circ \times \pm 10.0^\circ$	1852	0.86	0.74	1.27
C8	Within area of $\pm 7.5^\circ \times \pm 22.5^\circ$	2799	0.85	0.72	1.25

3  
 4 **Table 9.** Comparison of collocation methods C4 versus C8 using ACOS, NIES, PPDF, RemoTeC, and  
 5 UoL GOSAT products near the Darwin site.

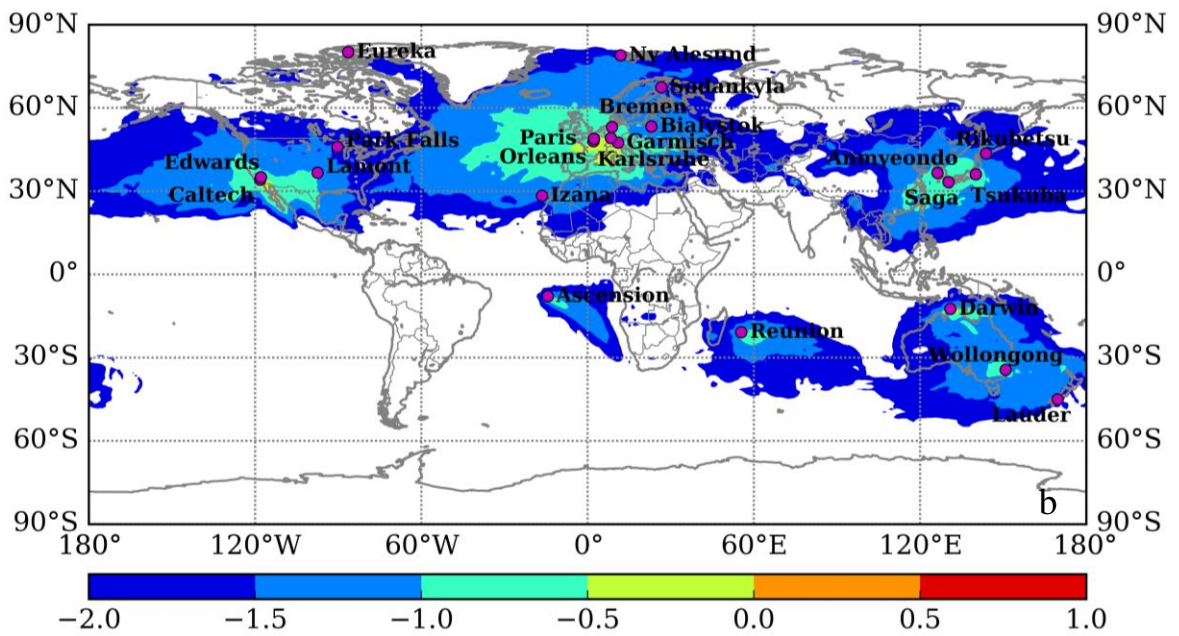
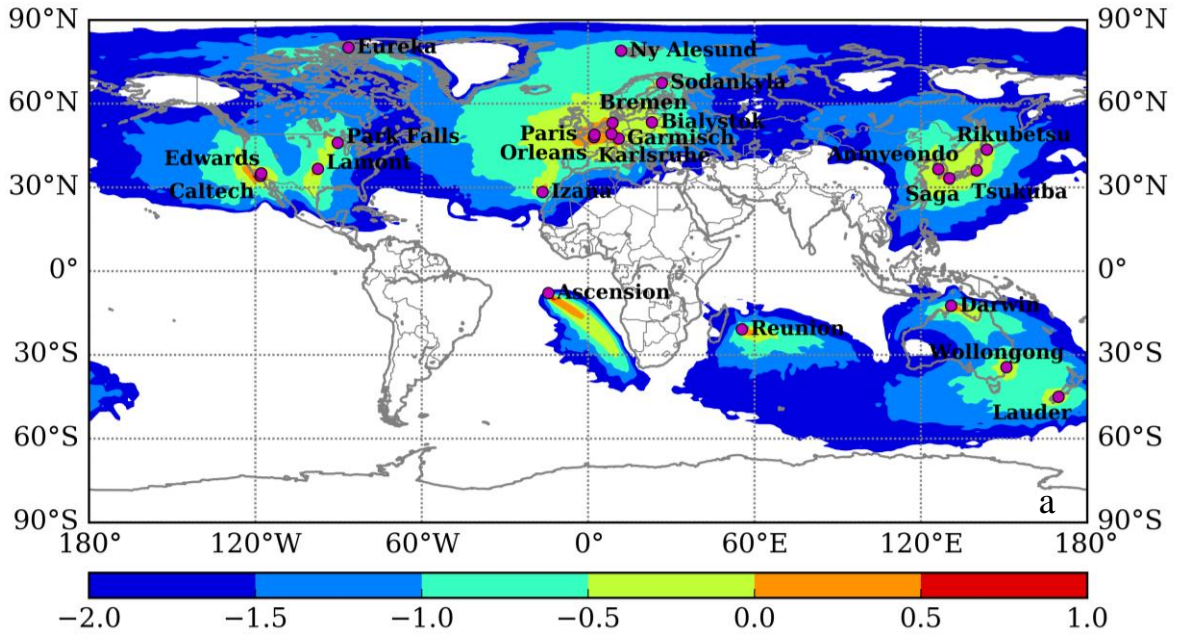
GOSAT Product	Case	Correlation coefficient	Mean bias	Standard deviation	Number of observations
ACOS	C4	0.96	0.36	0.77	36292
	C8	0.94	0.50	0.90	10872
NIES	C4	0.94	0.09	0.88	26652
	C8	0.93	0.13	1.00	6924
PPDF	C4	0.70	0.24	1.02	13681
	C8	0.64	0.08	1.10	4333
RemoTeC	C4	0.91	0.44	0.95	23915
	C8	0.89	0.77	1.07	7130
UoL	C4	0.82	0.34	1.17	14376
	C8	0.86	0.17	1.10	4727

6 **Table 10.** Comparison of collocation methods C4 versus C8 using ACOS, NIES, RemoTeC, and UoL  
 7 GOSAT products near the La Réunion site. The PPDF GOSAT product does not include any  
 8 observations near the La Réunion site.

GOSAT Product	Case	Correlation coefficient	Mean bias	Standard deviation	Number of observations
ACOS	C4	0.82	0.70	0.83	11873
	C8	0.83	0.65	0.76	9640
NIES	C4	0.70	0.25	1.07	7720
	C8	0.73	0.45	1.02	6505
RemoTeC	C4	0.51	0.92	1.07	2482
	C8	0.61	1.16	1.04	3414
UoL	C4	0.45	0.75	0.94	860
	C8	0.36	0.71	1.00	2239

9

1



3

4

5

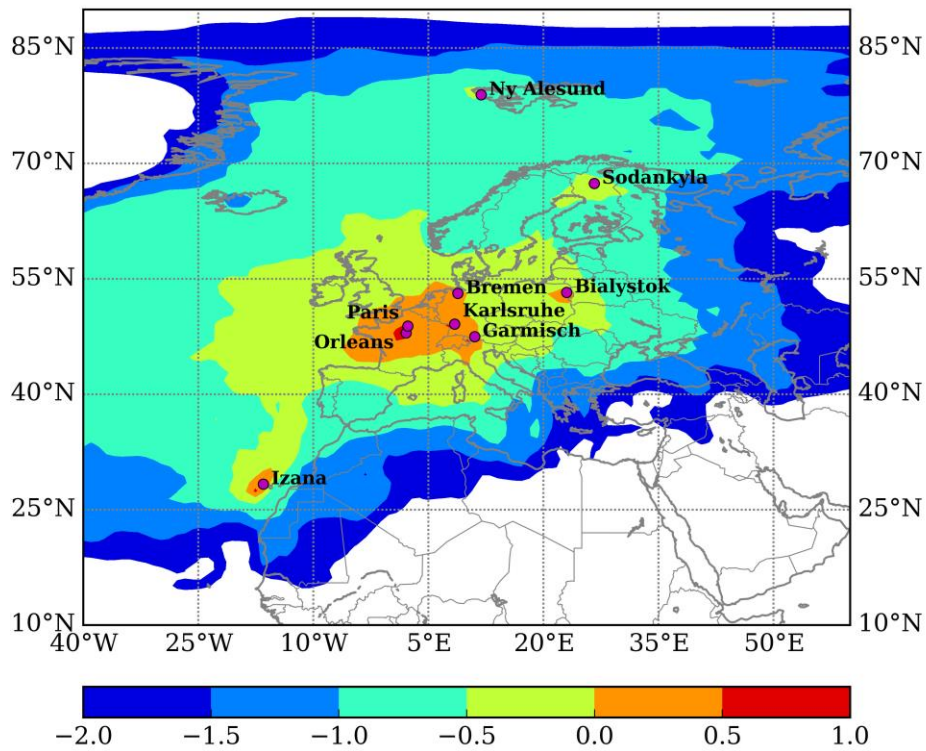
6

7

8

9

**Fig. 1.** Global distribution of the sensitivity of CO<sub>2</sub> concentrations (ppm (μmol (m<sup>2</sup>s)<sup>-1</sup>)<sup>-1</sup>) with respect to the concentrations in adjacent cells, calculated using the FLEXPART model with a resolution of 1.0° for the 23 TCCON operational sites: a) tracer simulation initialized at the level of 1000 m, b) tracer simulation initialized at the level of 3000 m that corresponds to 700 hPa based on the International Standard Atmosphere for dry air.



1

2

3

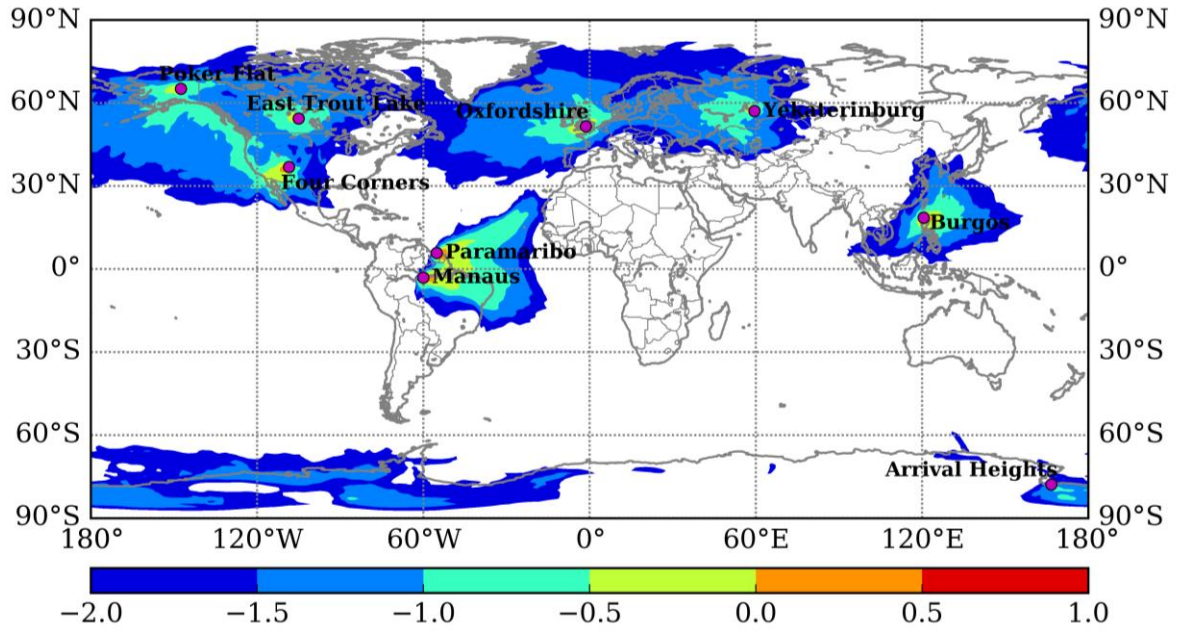
4

5

6

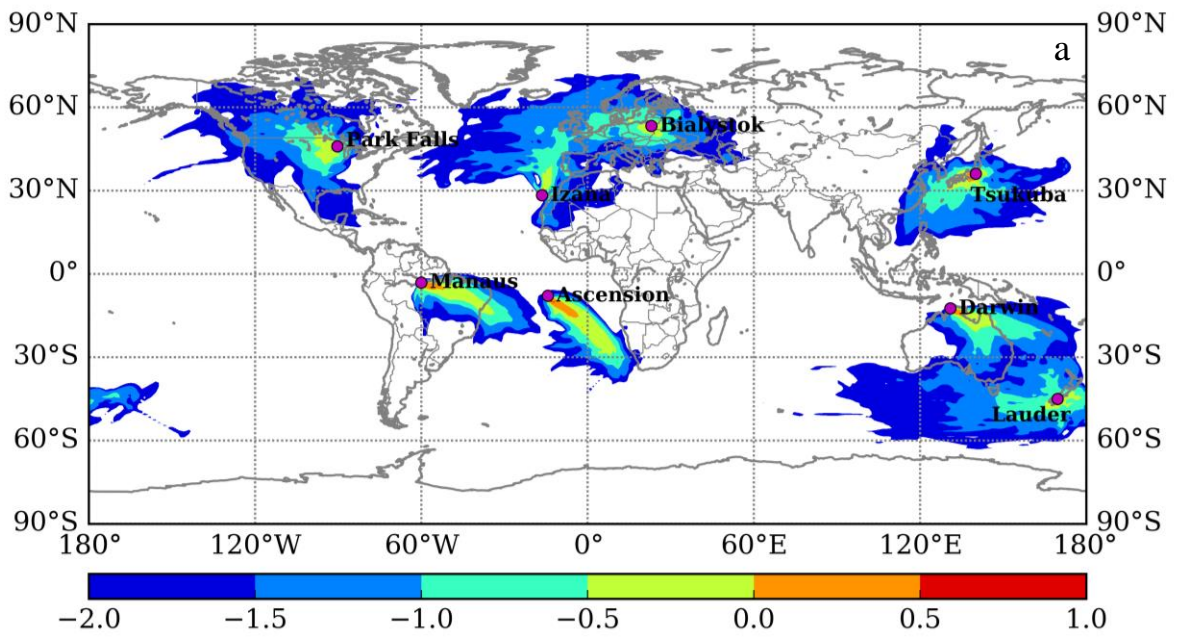
**Fig. 2.** Distribution of the sensitivity of CO<sub>2</sub> concentrations ( $\text{ppm} (\mu\text{mol} (\text{m}^2\text{s})^{-1})^{-1}$ ) in Europe with respect to the concentrations in adjacent cells, calculated using the FLEXPART model with a resolution of 1.0° for TCCON operational sites within Europe, using a tracer simulation initialized at the level of 1000 m.

1

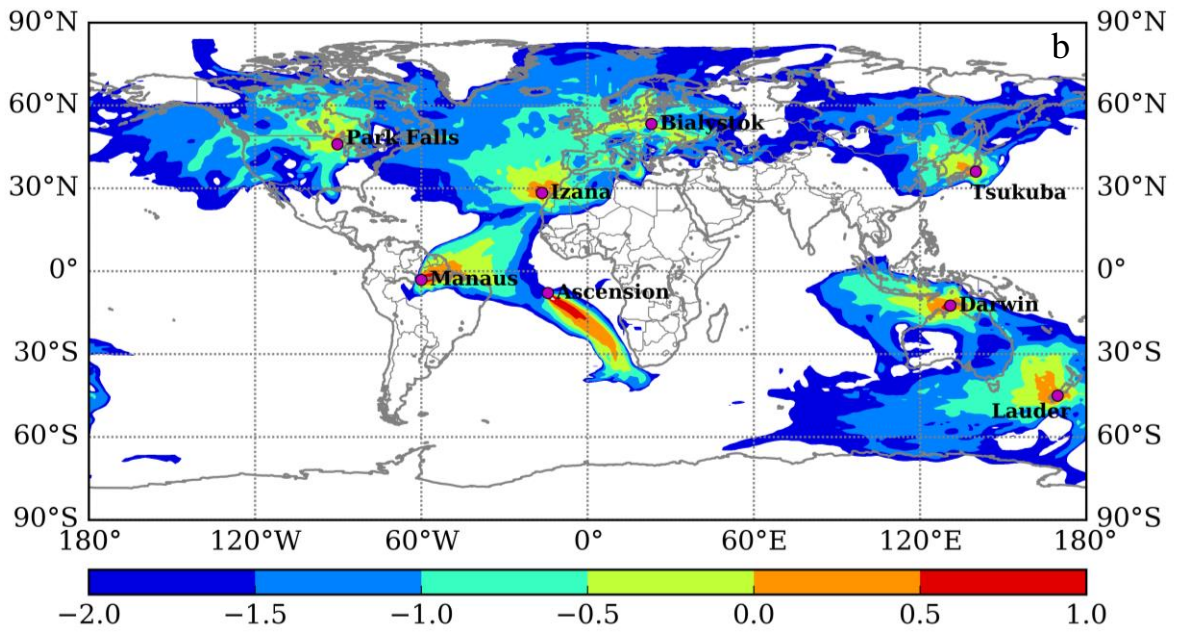


2

3 **Fig. 3.** Global distribution of the sensitivity of CO<sub>2</sub> concentrations (ppm (μmol (m<sup>2</sup>s)<sup>-1</sup>)<sup>-1</sup>) with  
4 respect to the concentrations in adjacent cells, calculated using the FLEXPART model with a  
5 resolution of 1.0° for 9 past, future, and possible TCCON operational sites, using a tracer  
6 simulation initialized at the level of 1000 m.  
7



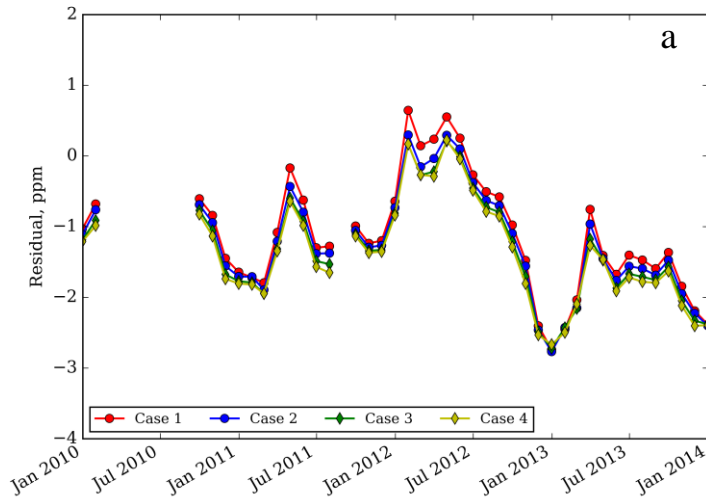
1  
2



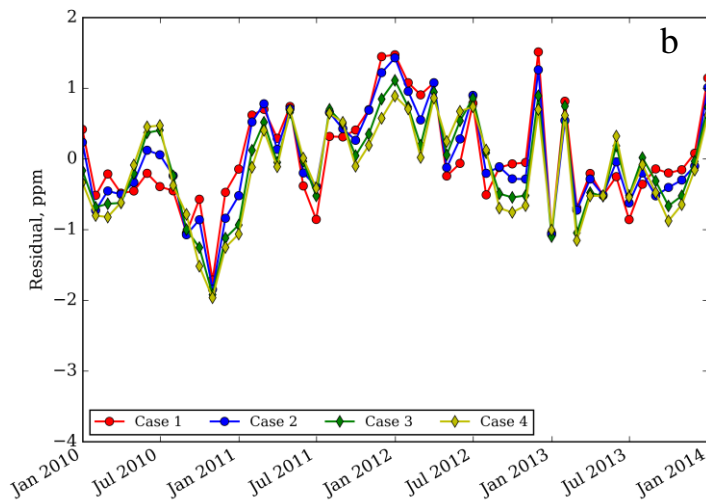
3

4 **Fig. 4.** Footprints for different seasons for Ascension Island, Białystok, Darwin, Izaña, Manaus,  
 5 Park Falls, and Tsukuba, for a) the summer (June, July, and August) of 2010 and b) the  
 6 winter (December, January, February) of 2010–2011.

7



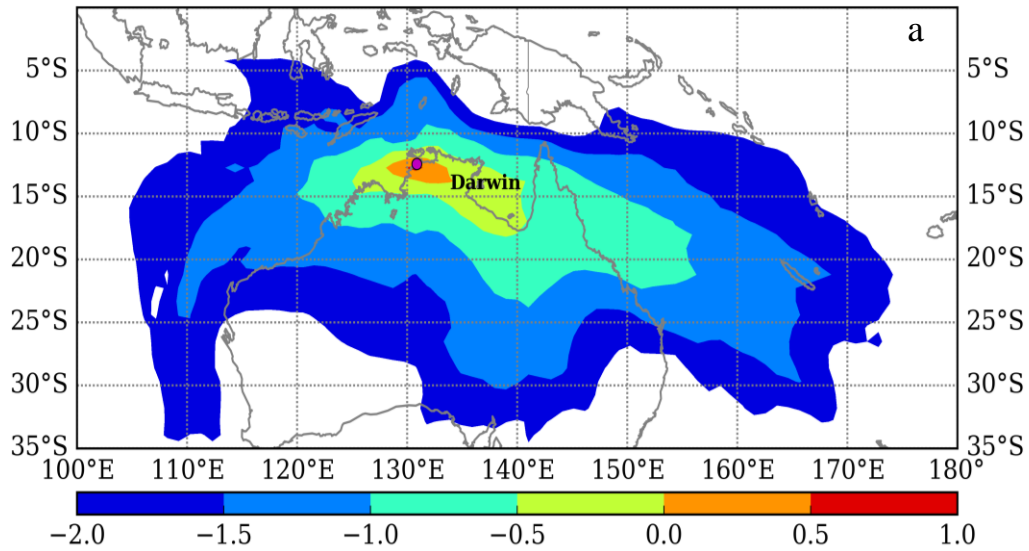
1



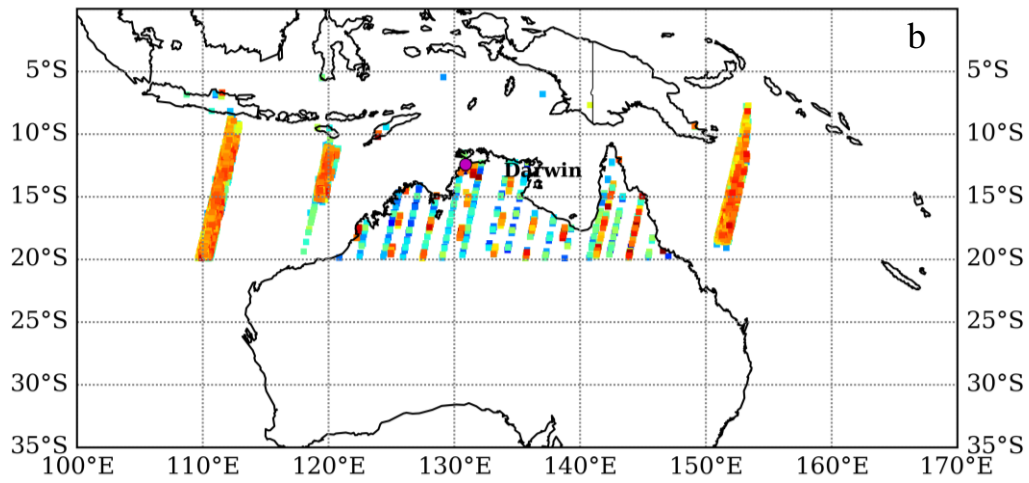
2

3 **Fig. 5.** Monthly average residuals of modeled XCO<sub>2</sub> compared with TCCON ground-based FTS for  
 4 methods C1, C4, C5 and C8, for a) Darwin and b) Garmisch.

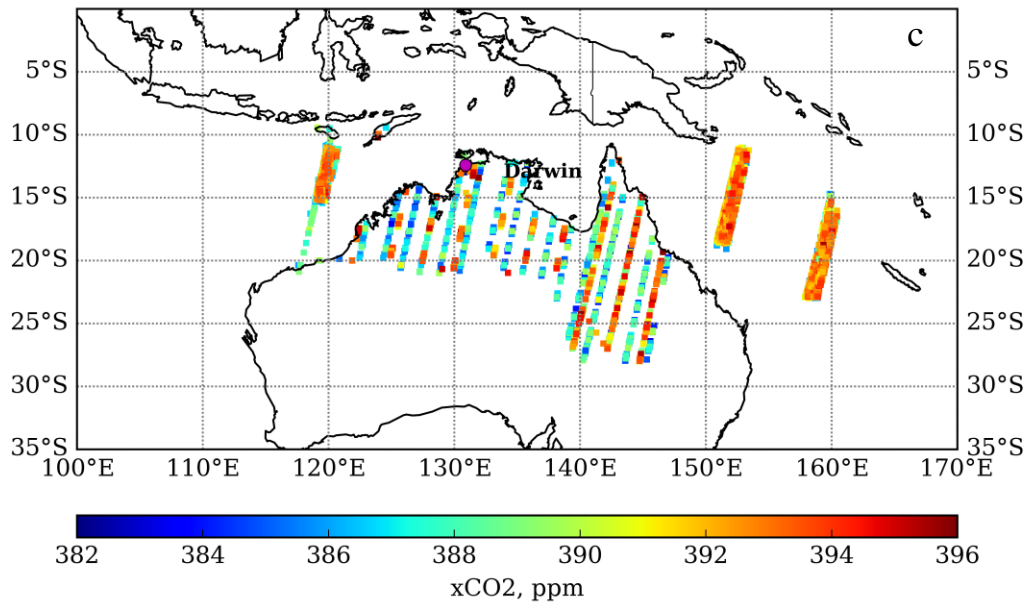
5



1  
2



3

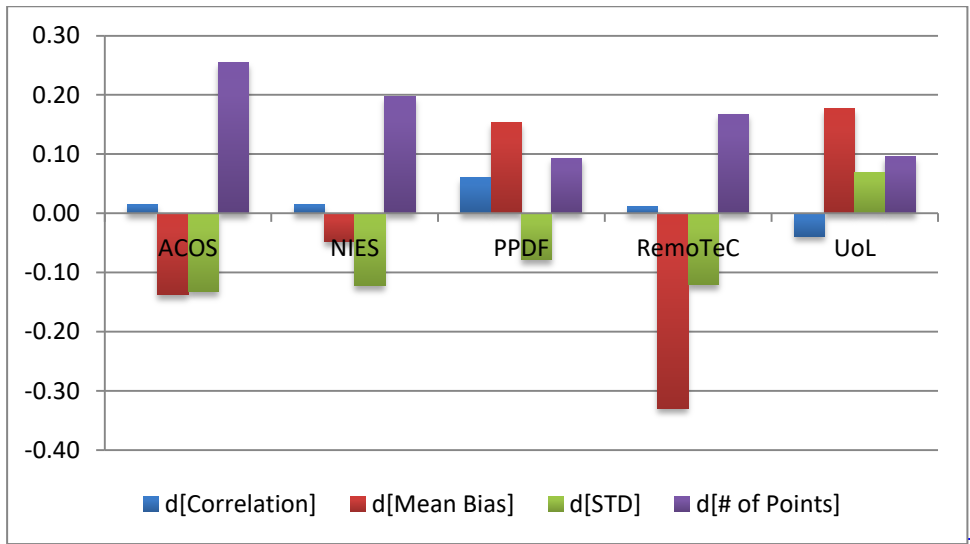


4

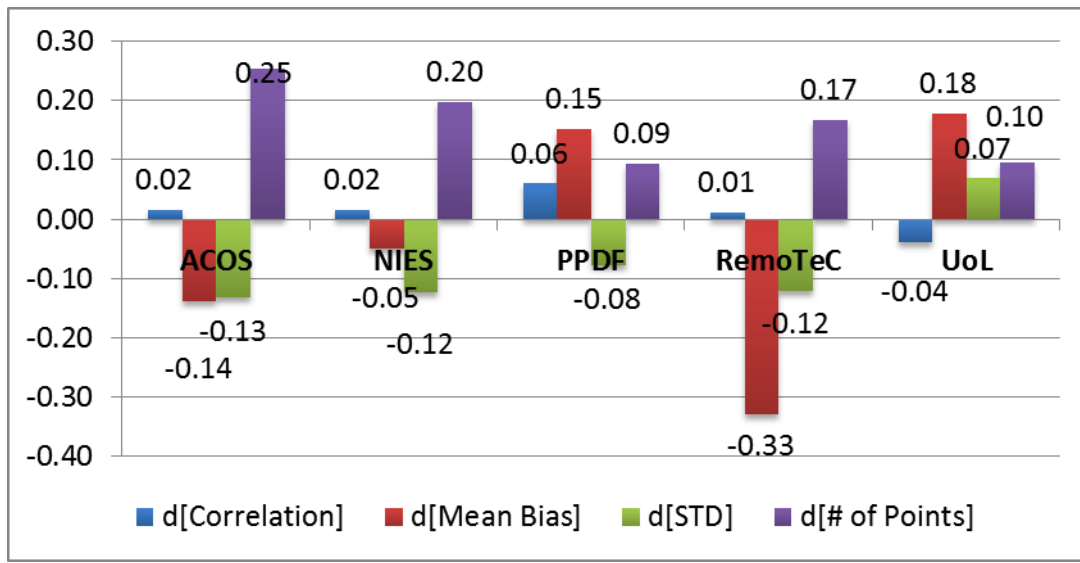
5 **Fig. 6.** a) Annual average footprint for the Darwin TCCON observation site; ACOS GOSAT XCO<sub>2</sub>  
 6 observations selected using b) the geostatistical method within an area of  $\pm 7.5^\circ \times \pm 22.5^\circ$ ,  
 7 and c) the footprint-based method with the limit  $\log_{10}(x) = -2.0$ .

8

1

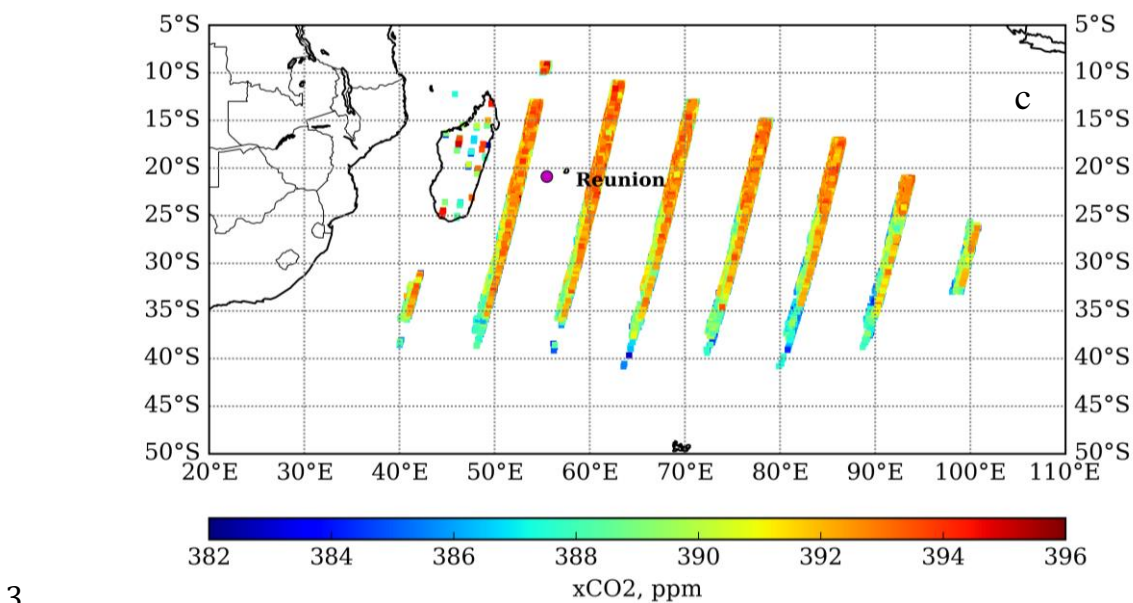
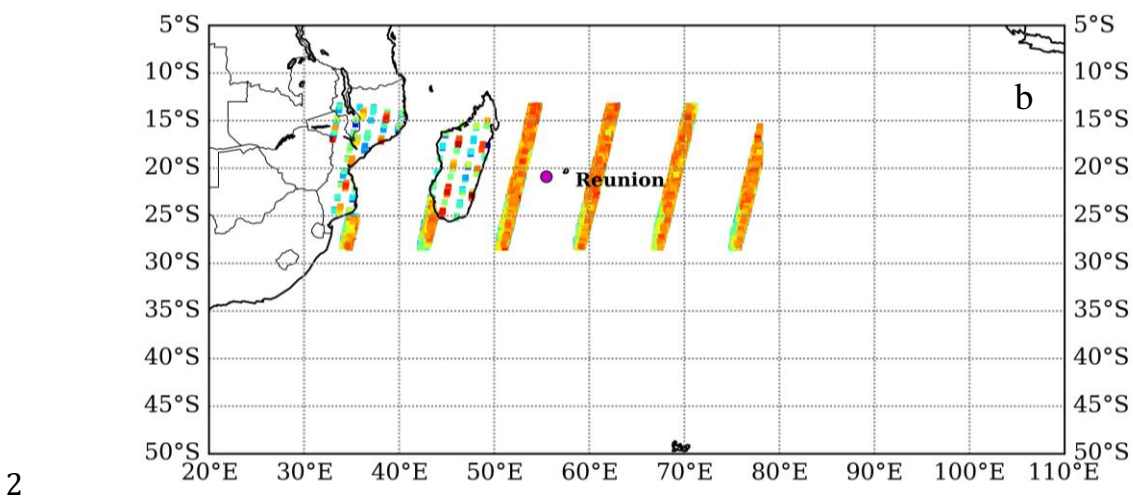
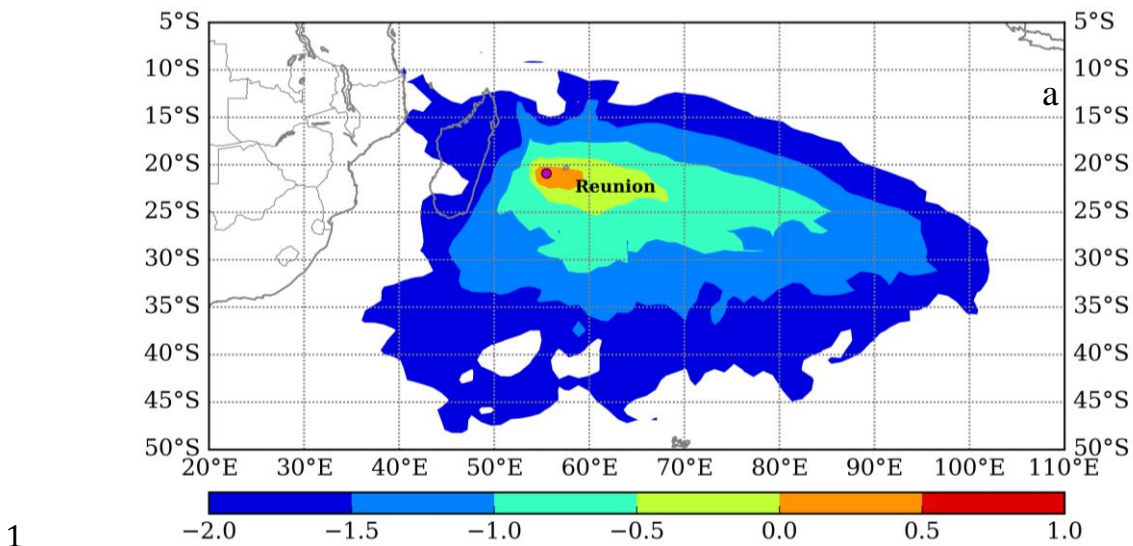


2



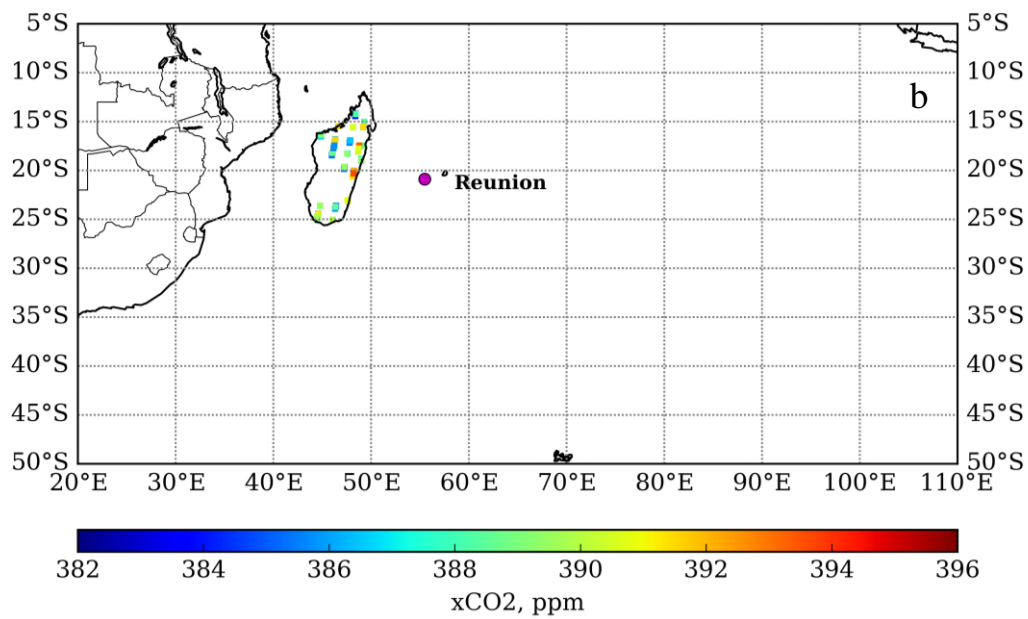
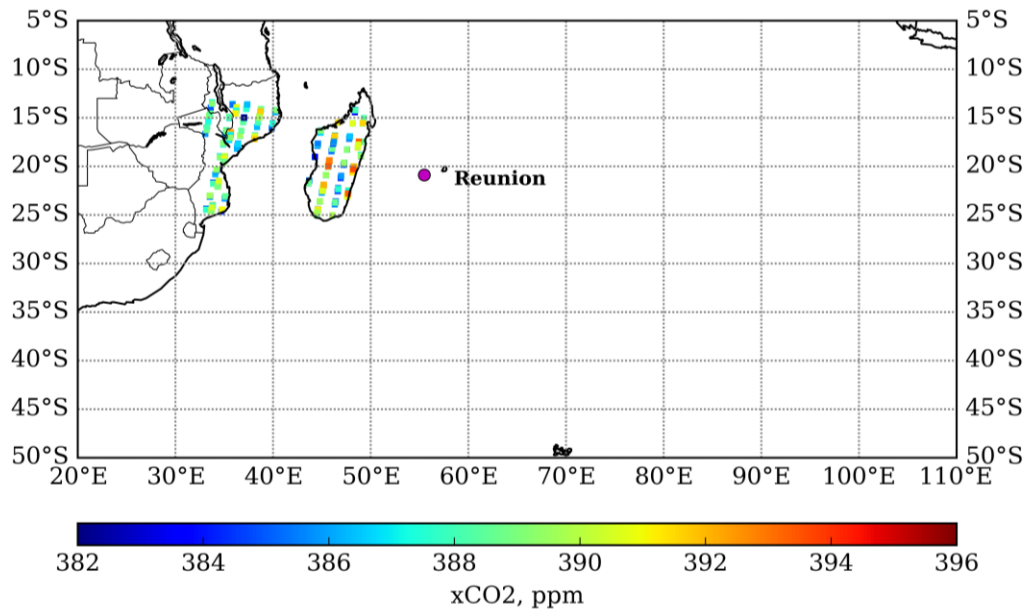
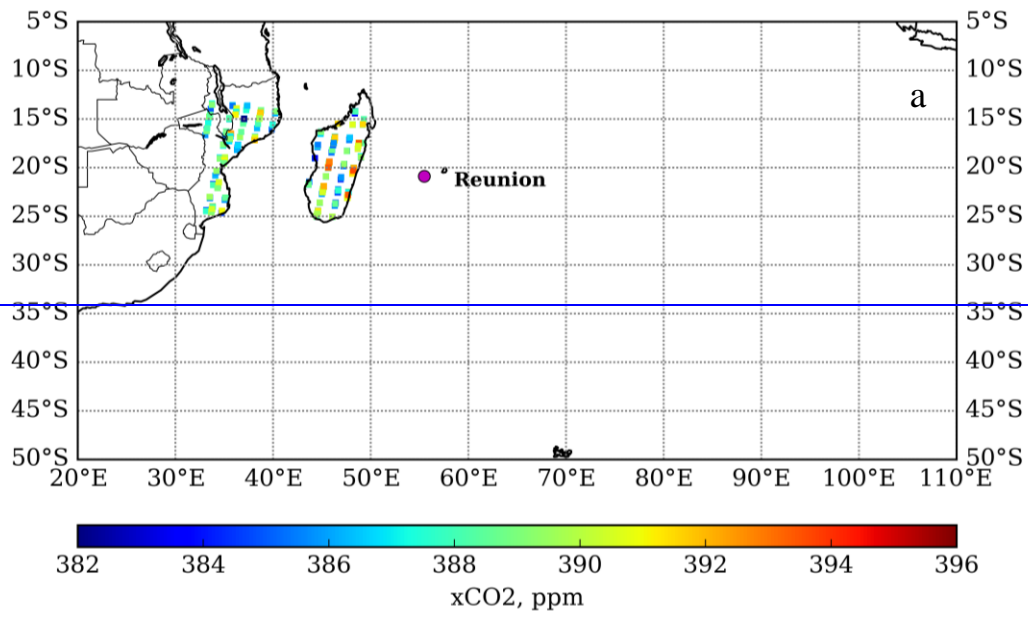
3 **Fig. 7.** Difference (denoted as d[ ]) in correlation coefficients, mean bias (ppm), STD (ppm) and  
 4 number of observational points between methods C4 ~~and C8~~ (the colocation domain size is  
 5 determined by sensitivity values (ppm (μmol (m<sup>2</sup>s)<sup>-1</sup>)<sup>-1</sup>) with the limit of log<sub>10</sub>(x) equal to -  
 6 2.0) and C8 (the colocation domain size is rectangular with dimension ±7.5° × ±22.5°) using  
 7 ACOS, NIES, PPDF, RemoTeC, and UoL GOSAT products near the Darwin site. Please note  
 8 scale of number of observational points is 10<sup>5</sup>.  
 9





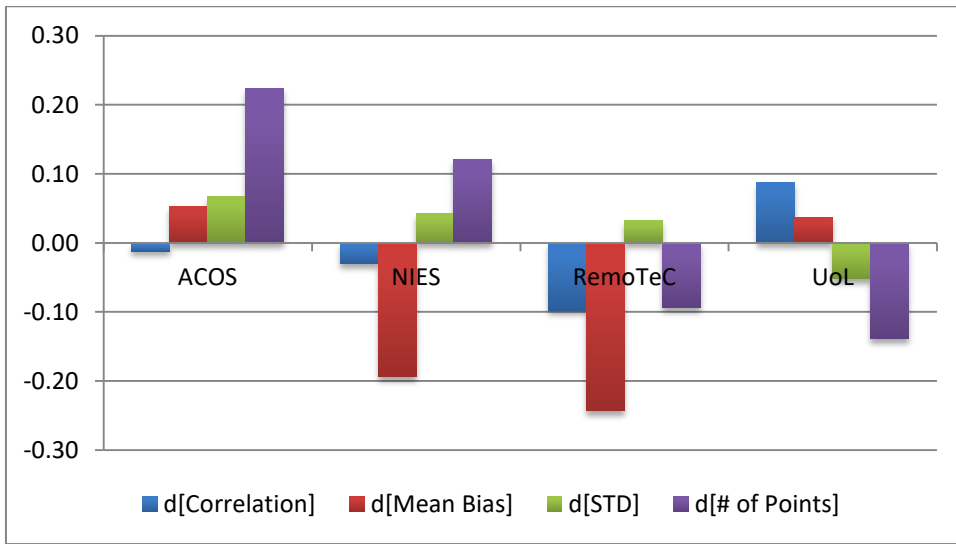
4 **Fig. 8.** a) Annual average footprint for the La Réunion TCCON observation site; ACOS GOSAT XCO<sub>2</sub>  
 5 observations selected using b) the geostatistical method within an area of  $\pm 7.5^\circ \times \pm 22.5^\circ$ ,  
 6 and c) the footprint-based method with the limit  $\log_{10}(x) = -2.0$ .

7

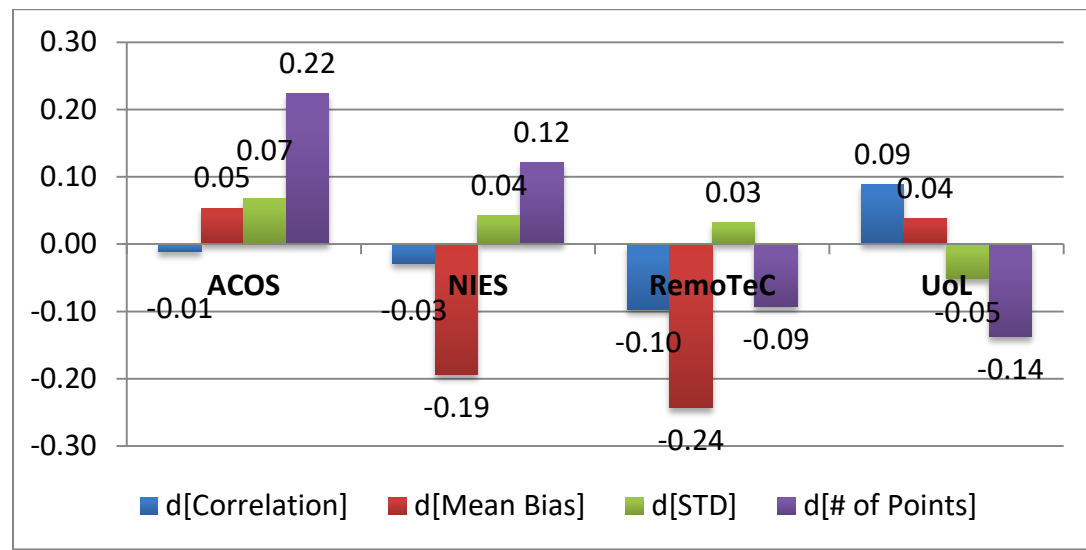


1 **Fig. 9.** UoL-FP GOSAT XCO<sub>2</sub> observations selected using a) the geostatistical method within an  
2 area of  $\pm 7.5^\circ \times \pm 22.5^\circ$ , and b) the footprint-based method with the limit  $\log_{10}(x) = -2.0$ .  
3

1



2



3 **Fig. 10.** Difference (denoted as d[]) in correlation coefficients, mean bias (ppm), STD (ppm)  
 4 and number of observational points between methods C4 and C8 (the colocation domain  
 5 size is determined by sensitivity values (ppm (μmol (m<sup>2</sup>s)<sup>-1</sup>)<sup>-1</sup>) with the limit of log<sub>10</sub>(x)  
 6 equal to -2.0) and C8 (the colocation domain size is rectangular with dimension ±7.5° ×  
 7 ±22.5°) using ACOS, NIES, RemoTeC, and UoL GOSAT products near the La Réunion site.  
 8 Please note scale of number of observational points is 10<sup>4</sup>.  
 9